Neuron, Vol. 35, 489–505, August 1, 2002, Copyright ©2002 by Cell Press

Regulation of AChR Clustering by Dishevelled Interacting with MuSK and PAK1

Zhen G. Luo,[1,10] Qiang Wang,[1,3,10] Jian Z. Zhou,[4] Jianbo Wang,[5] Zhijun Luo,[6] Mingyao Liu,[7] Xi He,[8] Anthony Wynshaw-Boris,[5] Wen C. Xiong,[2] Bai Lu,[4] and Lin Mei[1,9]

[1]Department of Neurobiology
Department of Pathology and
Department of Physical Medicine and Rehabilitation
Civitan International Research Center
[2]Department of Pathology
University of Alabama at Birmingham
1530 Third Avenue South
Birmingham, Alabama 35294
[3]Institute of Neuroscience
Shanghai Institutes of Biological Sciences
Chinese Academy of Sciences
Shanghai 200031
China
[4]Unit on Synapse Development and Plasticity
Laboratory of Developmental Neurobiology
NICHD
National Institutes of Health
Bethesda, Maryland 20892
[5]Department of Pediatrics and Medicine and
UCSD Cancer Center
School of Medicine
University of California, San Diego
9500 Gilman Drive
La Jolla, California 92093
[6]Diabetes and Metabolism Research Unit
Endocrinology Section
Evans Department of Medicine and
Department of Biochemistry
Boston University School of Medicine
Boston, Massachusetts 02118
[7]Institute of Biosciences and Technology
Department of Medical Biochemistry and Genetics
Texas A&M University System Health Science Center
Houston, Texas 77030
[8]Division of Neuroscience
Children's Hospital/Harvard Medical School
300 Longwood Avenue
Boston, Massachusetts 02115

Summary

An important aspect of synapse development is the clustering of neurotransmitter receptors in the postsynaptic membrane. Although MuSK is required for acetylcholine receptor (AChR) clustering at the neuromuscular junction (NMJ), the underlying molecular mechanisms remain unclear. We report here that in muscle cells, MuSK interacts with Dishevelled (Dvl), a signaling molecule important for planar cell polarity. Disruption of the MuSK-Dvl interaction inhibits Agrin- and neuron-induced AChR clustering. Expression of dominant-negative Dvl1 in postsynaptic muscle cells reduces the amplitude of spontaneous synaptic currents at the NMJ. Moreover, Dvl1 interacts with downstream kinase PAK1. Agrin activates PAK, and this activation requires Dvl. Inhibition of PAK1 activity attenuates AChR clustering. These results demonstrate important roles of Dvl and PAK in Agrin/MuSK-induced AChR clustering and reveal a novel function of Dvl in synapse development.

[9]Correspondence: lmei@nrc.uab.edu
[10]These authors contributed equally to this work.

Introduction

The neuromuscular junction (NMJ) is a synapse between motoneurons and skeletal muscle fibers that exhibits the high degree of subcellular specialization characteristic of chemical synapses (Hall and Sanes, 1993; Sanes and Lichtman, 1999, 2001). Due to its relative simplicity and accessibility, the NMJ has been studied extensively as a model of synaptogenesis. A signature of the NMJ is the high concentration of synaptic proteins including acetylcholine receptors (AChRs) in the postsynaptic membrane that guarantees fast and accurate neurotransmission (Burden, 1998; Colledge and Froehner, 1998; Fallon and Hall, 1994; Sanes and Lichtman, 2001). In the absence of innervation, the muscle seems to be prepatterned (Ferns and Carbonetto, 2001; Lin et al., 2001; Yang et al., 2001, 2000). Small AChRs clusters aggregate in the central region of the muscle, forming a central band that appears to be wider and more poorly defined than in innervated muscle. Upon innervation, AChR clusters are restricted to a narrow central band. Studies of regenerating synapses demonstrate that the synaptic basal lamina contains a signal to cause redistribution of AChRs (McMahan et al., 1992). This signal is believed to be Agrin, a 200 kDa polypeptide that is expressed in motoneurons, transported to presynaptic nerve terminals, and deposited in the basal lamina in the synaptic cleft. Neural Agrin induces postsynaptic differentiation in cultured muscle cells (Campanelli et al., 1991; Tsim et al., 1992; Wallace, 1989). Studies of mutant mice convincingly demonstrate that Agrin is essential for AChR clustering in the membrane opposite the presynaptic terminals (Gautam et al., 1996; Ruegg and Bixby, 1998).

MuSK, a receptor tyrosine kinase, was discovered because of its abundance in the synapse-rich *Torpedo* electric organ, whose principal cells are modified muscle cells that are innervated by cholinergic synapses (Jennings et al., 1993). Studies of the MuSK mouse homolog reveal that MuSK is specifically expressed in skeletal muscles and is colocalized with AChRs in the postsynaptic membrane at the NMJ (Valenzuela et al., 1995). Agrin activates MuSK, and expression of a dominant-negative form of MuSK inhibits Agrin-induced cluster formation in cultured myotubes (Glass et al., 1996). The extracellular domain of MuSK inhibits Agrin-induced AChR clustering in C2C12 muscle cells (Glass et al.,

1996). Moreover, *MuSK*$^{-/-}$ mice fail to form the NMJ (DeChiara et al., 1996; Lin et al., 2001; Yang et al., 2001). Agrin was unable to induce AChR clustering in muscle cells of MuSK mutant mice (Glass et al., 1996), but Agrin sensitivity was restored by introduction of wild-type MuSK into *MuSK*$^{-/-}$ myotubes (Herbst and Burden, 2000; Zhou et al., 1999). These results demonstrate that MuSK is essential for Agrin-induced AChR clustering. However, the intracellular signaling mechanisms downstream of MuSK are poorly understood. Agrin induces tyrosine phosphorylation of AChR β and δ subunits, probably via an Src-like kinase (Ferns et al., 1996; Fuhrer and Hall, 1996; Qu and Huganir, 1994; Wallace et al., 1991). It is thought that tyrosine phosphorylation facilitates the interaction of AChRs with cytoskeletal proteins such as F-actin (Dai et al., 2000) and/or reduces the solubility of tyrosine-phosphorylated AChR (Borges and Ferns, 2001; Ferns and Carbonetto, 2001; Fuhrer and Hall, 1996; Mohamed et al., 2001). Studies of mutant mice indicate that Src, Fyn, and Yes are not required for the formation of AChR clusters but are necessary for stabilization of Agrin-induced clusters (Smith et al., 2001). In a recent study, Agrin has been shown to activate Rho GTPase Rac and Cdc42, and these molecules are required for Agrin-induced AChR clustering in cultured muscle cells (Weston et al., 2000). In addition, these processes may be regulated by intracellular calcium, which is required for the induction and maintenance of AChR clusters by Agrin (Borges et al., 2002; Megeath and Fallon, 1998; Wallace, 1988). While these studies begin to piece together signaling pathways that lead to AChR clustering, exactly how signals are transduced from MuSK to downstream molecules remains unclear.

To gain insight into molecular mechanisms of Agrin signaling leading to AChR clustering, we searched for proteins that interact with MuSK. We identified Dishevelled-1 (Dvl1) as a MuSK binding partner. Dishevelled (Dsh/Dvl) was originally discovered in *Drosophila* for its role in the development of coherent arrays of polarized cells (Perrimon and Mahowald, 1987). Complete loss of Dsh produces a segment polarity defect indistinguishable from that seen in wingless (Perrimon and Mahowald, 1987). In the canonical pathway, Wnt binds to and activates its receptor, the Frizzled family of seven transmembrane domain proteins (Bhanot et al., 1996; Cadigan and Nusse, 1997; Malbon et al., 2001). This signal is transmitted through Dsh/Dvl, which inhibits phosphorylation of β-catenin (or Arm for armadillo) by glycogen synthase kinase 3β (GSK3 or Zw-3). The net result is the upregulation of β-catenin and its translocation into the nucleus, where it leads to activation of T cell factor (TCF)/LEF-1-dependent transcription (Cadigan and Nusse, 1997; Dale, 1998; Klingensmith et al., 1994; Noordermeer et al., 1994; Theisen et al., 1994). Dsh also participates in the planar cell polarity (PCP) pathway in *Drosophila* using components distinct from GSK3β, β-catenin, and dTCF (Axelrod et al., 1998; Boutros et al., 1998). Studies of genetic interactions indicate a role for RhoA downstream of Frizzled and Dsh for the generation of tissue polarity (Strutt et al., 1997). In addition, Dvl proteins, when expressed in heterologous cells, stimulate c-Jun-dependent transcription activity and the kinase activity of the c-Jun N-terminal kinase (JNK) (Boutros et al., 1998; Li et al., 1999). These results suggest that Dvl may act as a functional switch between distinct downstream pathways.

In this study, we explored the function of Dvl in Agrin/MuSK signaling. We have examined the effect of the disruption of the MuSK-Dvl interaction on Agrin-induced AChR clustering in muscle cells as well as AChR clustering in *Xenopus* nerve-muscle cocultures. The role of Dvl in Agrin-induced AChR clustering has also been characterized using an antisense DNA approach. Finally, we investigated downstream mechanisms of Dvl. These studies identified a critical signaling mechanism downstream of MuSK important for AChR clustering and revealed a novel function of Dvl in synaptogenesis.

Results

Dishevelled Interacts with MuSK via the DEP Domain

To identify MuSK-interacting proteins that may participate in or regulate Agrin signaling, we used the yeast two-hybrid system as described previously (Huang et al., 2000). A screen of mouse cDNA libraries (Lumeng et al., 1999) using as bait the entire cytoplasmic region of MuSK (MuSKic, aa 517–871) led to the finding of Dvl1. The original clone encoded mouse Dvl1 (aa 181–695) with a deletion of the N-terminal 180 amino acids. Dvls are cytoplasmic proteins consisting of three conserved domains: DIX (Dishevelled-Axin), PDZ, and DEP (Dishevelled-Egl-10-Pleckstrin) (Cadigan and Nusse, 1997; Dale, 1998). The isolated clone covered only PDZ and DEP, suggesting that DIX is not required for interaction with MuSK (Figure 1A). Moreover, PDZ (aa 181–425) alone did not interact with MuSKic, although the MuSK C terminus contains a putative PDZ domain binding motif (Torres et al., 1998). In contrast, MuSK interacted with DEP (aa 380–695) in yeast (Figure 1A), suggesting that Dvl1 interacts with MuSK via DEP. To determine which region of MuSK interacts with Dvl, a series of MuSK mutants were characterized for binding to PDZ-DEP. Deletion of the C terminus had no effect on MuSK binding to Dvl, suggesting this region is not required. However, the interaction depended on the integrity of both the juxtamembrane and kinase domains since deletion of either domain abolished interaction (Figure 1B). The interaction of MuSK with Dvl was specific in that Dvl1 did not associate with ErbB4, a nonrelated receptor tyrosine kinase (Figure 1A).

To determine whether MuSK and Dvl1 interact in mammalian cells, we engineered an expression vector encoding Flag-tagged full-length MuSK in which the epitope was inserted after the signal peptide. Flag-MuSK was cotransfected into HEK 293 cells together with Myc-Dvl1. The two proteins coimmunoprecipitated (Figure 1C). This interaction was specific since coimmunoprecipitation of Dvl1 with the anti-Flag antibody was dependent on the expression of Flag-MuSK and the addition of anti-Flag antibody (Figure 1C). In a typical coimmunoprecipitation, ~3% of Dvl1 came down with MuSK (Figure 1C). Considering only ~50% of MuSK was immunoprecipitated, the amount of Dvl1 that interacted with MuSK was estimated to be ~6% in this experiment. These findings indicate that MuSK and Dvl1 interact with

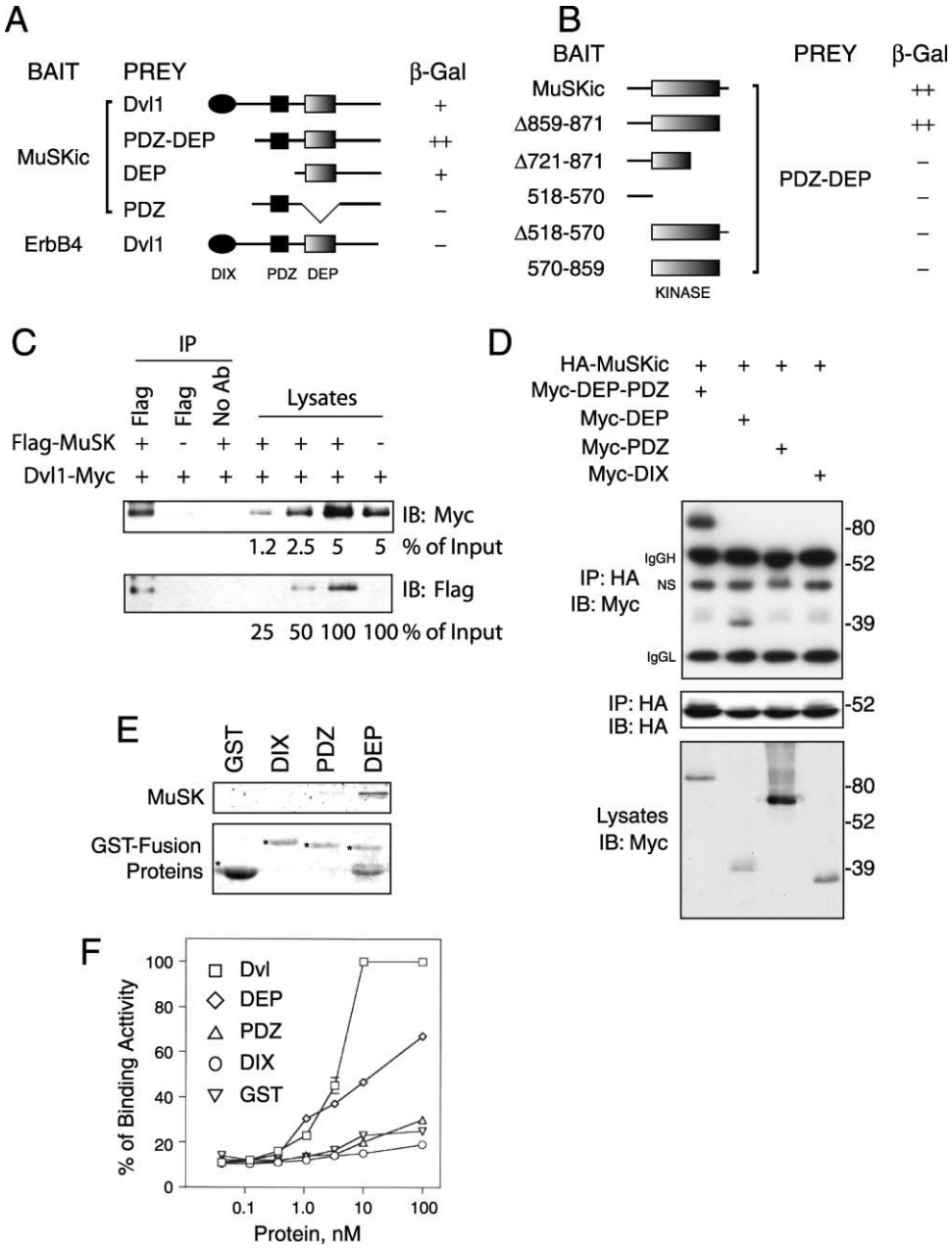

Figure 1. Interaction of MuSK with Dvl in Yeast and in Mammalian Cells

(A) Interaction of MuSK with Dvl via the DEP domain in yeast. Yeast cells were cotransformed with MuSKic in pGBT9 and indicated Dvl and ErbB4 constructs in pGAD424 or pACT2. Transformed yeast cells were seeded in $Leu^{-}Trp^{-}His^{-}$ plates and scored for β-gal activity. The original clone isolated from the library was PDZ-DEP.

(B) Dependence of the MuSK-Dvl interaction on the juxtamembrane domain and kinase domain. Yeast cells were cotransformed with MuSKic or mutants in pGBT9 and PDZ-DEP in pACT2 and scored for β-gal activity.

(C) Coimmunoprecipitation of MuSK and Dvl1 in HEK293 cells. Immunoprecipitates with anti-Flag antibody were subjected to immunoblotting with indicated antibodies. Percentage of lysate inputs was immunoblotted to quantify the immunoprecipitation.

(D) DEP associates with MuSK in HEK293 cells. Interaction of HA-MuSKic and Myc-Dvl2 domains was analyzed by immunoprecipitation as described in (C). IgGH, IgG heavy chain; IgGL, IgG light chain; NS, nonspecific proteins.

(E) Direct interaction between MuSK and DEP in vitro. ^{35}S-labeled MuSK was incubated with 10 μg indicated Dvl1 GST fusion proteins. Bound MuSK was resolved on SDS-PAGE and exposed to X-ray film.

(F) ELISA analysis of the affinity between MuSK and Dvl1.

each other in HEK 293 cells. In addition to Dvl1, other murine isoforms (Dvl2 and Dvl3) interacted with MuSK, also in a manner dependent on DEP (Figure 1D, and our unpublished data).

To determine whether MuSK interacts directly with Dvl1 and not via a third component, recombinant MuSK was generated by in vitro translation. ^{35}S-labeled MuSK was incubated with Dvl1 GST fusion proteins immobi-

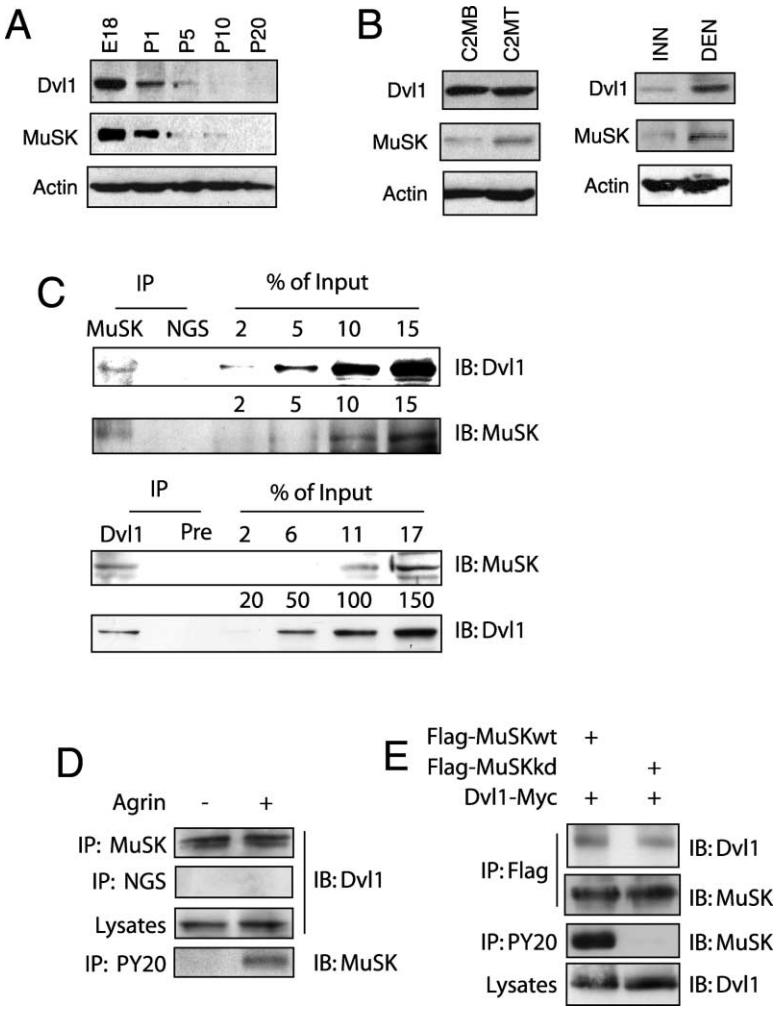

Figure 2. Expression of Dvl1 in Developing Muscles and In Vivo Dvl1-MuSK Interaction

(A) Expression of Dvl1 in developing muscles. Homogenates (50 μg of protein) were probed with antibodies against Dvl1, MuSK, or β-actin.

(B) Increased expression of Dvl1 in denervated muscles. Cell lysates of C2C12 myoblasts (MB) and myotubes (MT), or homogenates from adult muscles (normal [INN] or six days post denervation [DEN]) were subjected to immunoblotting as described in (A).

(C) Interaction between endogenous MuSK and Dvl1 in muscles. C2C12 myotube lysates (500 μg of protein) were incubated with either anti-MuSK or anti-Dvl1 antibodies. Resulting immunocomplexes were subjected to immunoblotting with reciprocal antibodies. Percentage of lysate inputs was immunoblotted to quantify the immunoprecipitation.

(D) Effect of Agrin on the MuSK-Dvl interaction in muscle cells. C2C12 myotubes were stimulated with Agrin or vehicle for 15 min. Immunoprecipitates with anti-MuSK antibody or normal goat serum (NGS) were probed with anti-Dvl1 antibodies. MuSK activation was shown by the increase in phosphotyrosine.

(E) Dvl interaction with kinase-inactive MuSK. HEK293 cells were cotransfected with Flag-MuSK or MuSKkd and Myc-Dvl1. Immunoprecipitates with anti-MuSK antibody were immunoblotted for Dvl.

lized on agarose beads. GST alone did not precipitate with MuSK, nor did GST-DIX or GST-PDZ (Figure 1E). In contrast, GST-DEP pulled down ^{35}S-labeled MuSK. Biochemically, the MuSK-Dvl1 interaction was dose dependent and saturable, with an EC50 value of 3.86 ± 0.26 nM in ELISA-based binding assays (Figure 1F). Of the Dvl1 mutants, only DEP was able to bind to MuSKic with similar affinity (1.44 ± 0.23 nM); binding of DIX or PDZ was barely detectable. Note that the maximal binding of Dvl is twice that of DEP, probably due to dimerization. Taken together, these results demonstrate that MuSK, via the juxtamembrane and kinase domains, interacts directly with the DEP domain of Dvl1.

Expression and Interaction of Dishevelled with MuSK in the Muscle

During development, Dvl1 was expressed at a high level in skeletal muscle at E18 and at birth, but the expression level decreased as development progressed (Figure 2A). This pattern was similar to that of MuSK (Figure 2A) (Valenzuela et al., 1995). In addition, Dvl1 was readily detectable in myoblasts as well as myotubes (Figure 2B). Denervation of skeletal muscles caused rapid degeneration of presynaptic nerves. Expression of postsynaptic proteins was normal or elevated to compensate the loss of presynaptic input (Tanowitz and Mei, 1996). While actin remained unchanged, expression of Dvl1

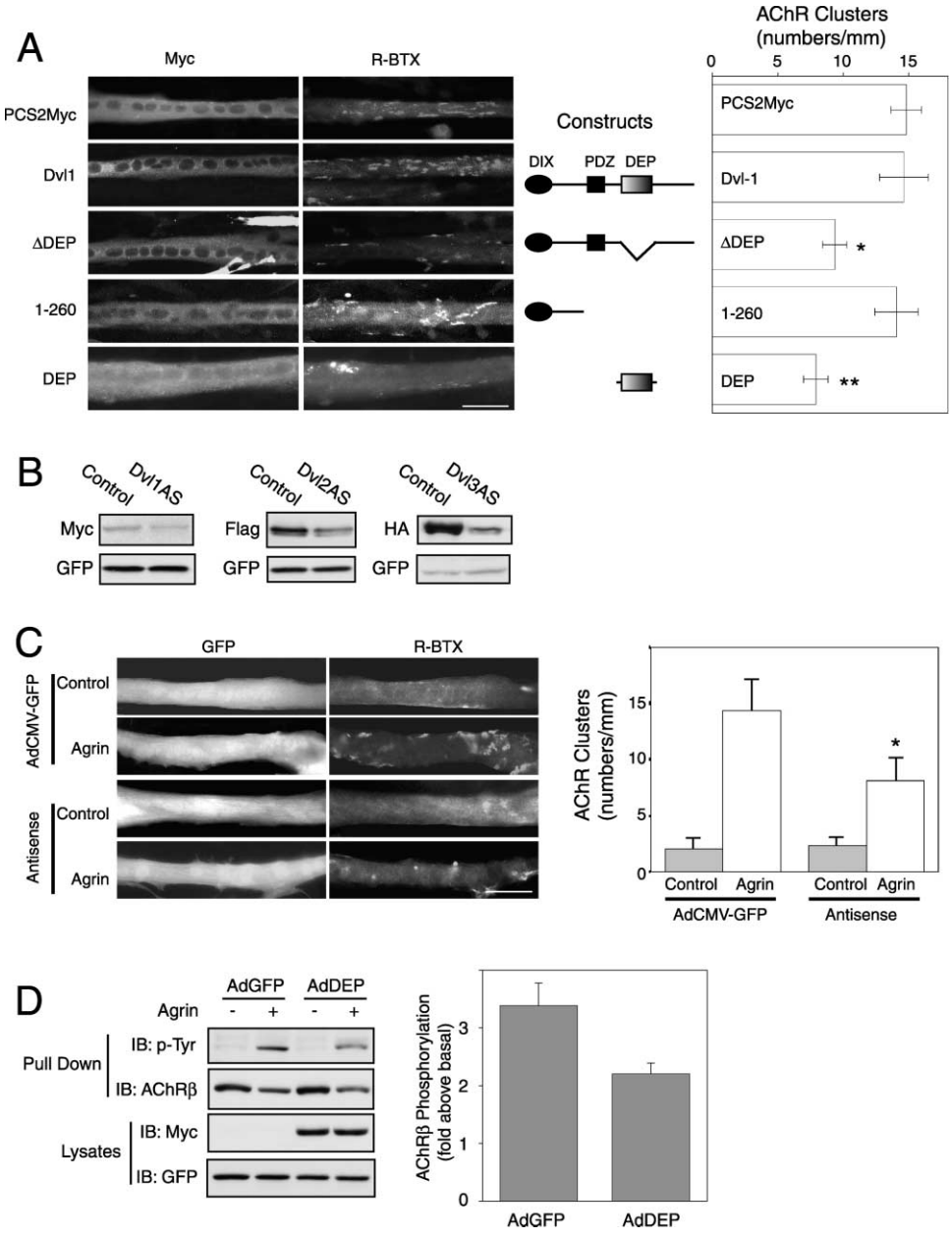

Figure 3. Inhibition of Agrin-Induced AChR Clustering by Dvl Mutants and in Dvl-Deficient Muscle Cells

(A) Inhibition of Agrin-induced AChR clusters in C2C12 myotubes by Dvl1 mutants. C2C12 myoblasts were transfected with indicated constructs and were induced to form myotubes 24 hr later. AChR clusters were assayed on Myc-positive myotubes as described in Experimental Procedures. Scale bar, 50 μm. The histogram summarizes data. PCS2Myc, n = 21; ΔDEP, n = 33; and DEP, n = 20. One-way ANOVA with Tukey HSD post hoc tests; *$p < 0.05$, **$p < 0.01$.

(B) Inhibition of Dvl isoform expression by antisense constructs. C2C12 cells were cotransfected with Dvl1-Myc, Flag-Dvl2, and HA-Dvl3, and antisense cDNAs in pAdEasy (see Experimental Procedures). Cell lysates were probed for Dvl isoforms with respective antibodies and GFP.

(C) Inhibition of Agrin-induced AChR clustering by Dvl antisense DNA constructs. GFP-positive myotubes were stained with R-BTX. Scale bar, 50 μm. Quantitative analyses of data are shown in the histogram. AdCMV-GFP: control, n = 20 and Agrin, n = 20. Antisense: control, n = 21 and Agrin, n = 20. Student's t test; *$p < 0.01$.

(D) Effect of DEP on tyrosine phosphorylation of the AChR β subunit. Purified AChRs from infected C2C12 myotubes were probed for tyrosine phosphorylation by HRP-conjugated RC20 antibody. Densitometric analyses of β subunit tyrosine phosphorylation (n = 3) are shown in the histogram.

was increased in denervated muscles (Figure 2B), supporting the notion that Dvl1 is a postsynaptic component. In addition, these results suggest that Dvl expression, like MuSK, is regulated by electric activity.

To determine whether Dvl1 and MuSK interact in vivo, we investigated whether MuSK could be coimmunoprecipitated with Dvl1 from the C2C12 muscle cells. Immunoprecipitation of MuSK resulted in coprecipita-

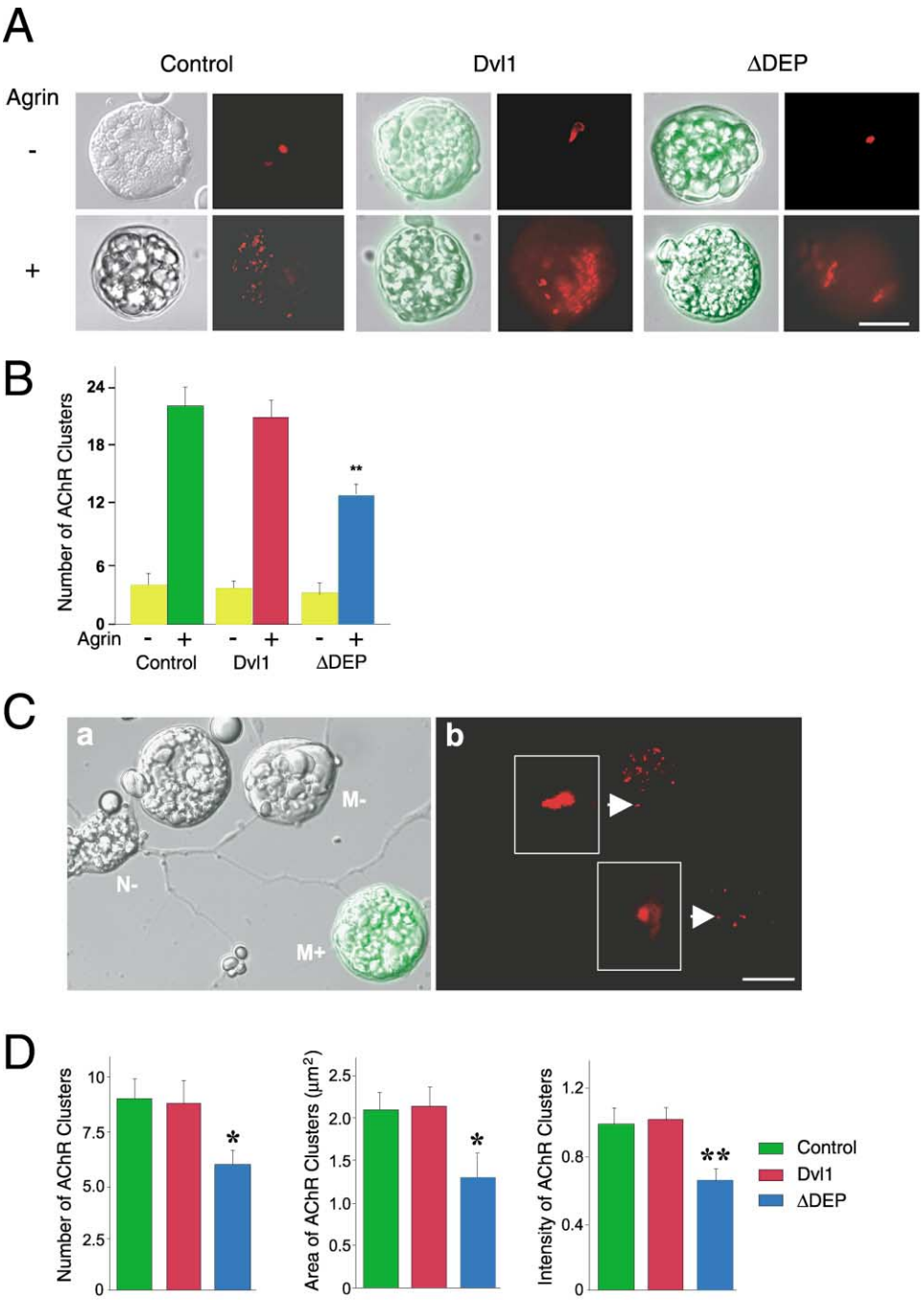

Figure 4. Inhibition of AChR Clustering at the NMJ by ΔDEP

(A) Inhibition of Agrin-induced AChR clustering. mRNAs for ΔDEP or Dvl1, together with GFP mRNAs, were expressed in isolated myocytes through embryo injection. Myocytes were treated with Agrin overnight. AChR clusters were visualized by R-BTX. Dvl1- or ΔDEP-expressing myocytes are indicated by GFP green fluorescence. Scale bar, 20 μm.

(B) Summary of the effects of ΔDEP and Dvl on AChR clusters in Agrin-treated isolated myocytes. Control, n = 17; Dvl, n = 15; ΔDEP, n = 17. ANOVA and post hoc test; **$p < 0.01$.

(C) Inhibition of AChR clustering at the NMJ. ΔDEP or Dvl1 were introduced into postsynaptic muscle cells through embryo injection. AChR clusters were measured in innervated myocytes in cultures without Agrin treatment. Nomarski and fluorescence images show a motoneuron (N) innervating two myocytes, one of which expresses ΔDEP (M+), as indicated by GFP. The same culture visualized using a rhodamine filter showing AChR clusters at the ΔDEP^- and ΔDEP^+ synapses. The clusters indicated by arrowheads are enlarged and shown in the insets. Scale bar, 20 μm.

(D) Summary of the effects of ΔDEP and Dvl on AChR clusters at the NMJ. Control, n = 20; Dvl, n = 18; ΔDEP, n = 18. ANOVA and post hoc test; *$p < 0.05$, **$p < 0.01$.

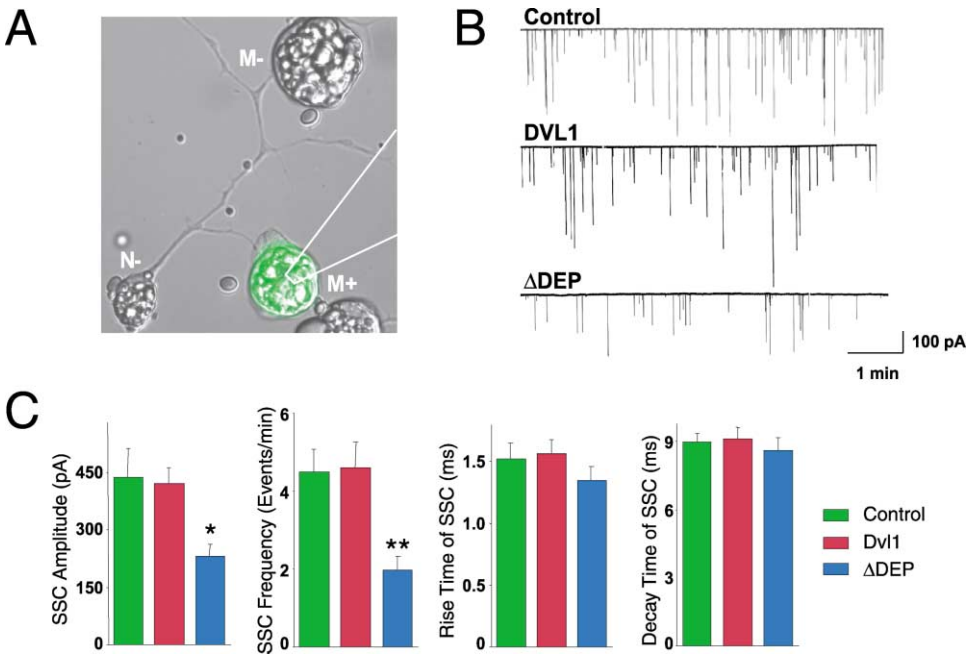

Figure 5. Inhibition of Synaptic Transmission at the NMJ by ΔDEP

SSCs were recorded in control, Dvl1, and ΔDEP^+ synapses under whole-cell, voltage-clamped conditions.

(A) Superimposed Nomarski and fluorescence images showing a motoneuron (N) innervating two myocytes, one of which expresses ΔDEP (M+), as indicated by GFP. The position of the electrode on a ΔDEP^+ myocyte is indicated.

(B) Three recording traces of SSCs (downward deflections of varying amplitudes) recorded from control, $Dvl1^+$, and ΔDEP^+ synapses.

(C) Summary of the effects of ΔDEP on SSCs. Control, n = 19; Dvl, n = 19; ΔDEP, n = 20. ANOVA and post hoc test; *$p < 0.05$, **$p < 0.01$.

tion of Dvl1 (Figure 2C). However, Dvl1 was undetectable in the precipitates by goat normal serum. Quantitatively, 3% of Dvl1 associated with 10% of MuSK that was precipitated; thus, 30% of Dvl1 in C2C12 myotubes interacts with MuSK. In reciprocal experiments, MuSK coprecipitated with Dvl1, and the amount of MuSK that interacts with Dvl1 is estimated to be 24% (Figure 2C). The coprecipitation of Dvl and MuSK seemed unaffected by Agrin (Figure 2D), suggesting that the MuSK-Dvl1 interaction may not be regulated by Agrin. In agreement, no apparent difference was noticed in Dvl binding to wild-type MuSK and to K608A (Figure 2E), a kinase-deficient mutant (MuSKkd) (Glass et al., 1997).

Involvement of Dvl in Agrin-Induced AChR Clustering

The temporal correlation of Dvl1 and MuSK expression and their interaction in vivo raise the possibility that Dvl1 is involved in Agrin/MuSK signaling. To test this, we determined whether Dvl or its mutants affect Agrin-induced AChR clustering in muscle cells. Transfected myotubes were identified by immunostaining with an anti-Myc antibody. AChR clusters were visualized with rhodamine-conjugated α-bungarotoxin (R-BTX). Expression of Dvl and its mutants had no detectable effect on basal AChR clustering (data not shown). Moreover, expression of Dvl1 appeared to have no detectable effect on Agrin-induced AChR clustering (Figure 3A). In contrast, ΔDEP, a Dvl mutant that did not interact with MuSK, inhibited the ability of Agrin to induce AChR clustering. The number of AChR clusters was decreased in ΔDEP-expressing cells, indicating that Agrin-induced AChR clustering involves the Dvl-MuSK interaction. To further test this concept, we studied the effect of DEP that interacts with MuSK. Overexpressed DEP may interfere with MuSK association with endogenous Dvl and thus inhibit AChR clustering. DEP attenuated Agrin-induced AChR clustering (Figure 3A). However, Dvl11-260 had no effect on Agrin-induced AChR clustering.

We next examined the effect of suppressing Dvl expression in C2C12 myotubes. All three Dvl homologs are expressed in skeletal muscles (Klingensmith et al., 1996; Sussman et al., 1994; Tsang et al., 1996). Antisense cDNAs (Dvl1, nt 1–184; Dvl2, nt 1–193; Dvl3, nt 1–183) of all three isoforms were subcloned individually in AdCMV-GFP (He et al., 1998). This vector encodes GFP under the control of a separate CMV promoter to allow easy identification of C2C12 myotubes expressing antisense constructs. Transfection of the three antisense constructs decreased expression of cotransfected Dvl isoforms in C2C12 cells by 50%–80% (Figure 3B). The empty AdCMV-GFP vector had no effect on basal or Agrin-induced AChR clusters. In addition, basal AChR clusters remained unchanged in C2C12 myotubes expressing antisense Dvl cDNAs. In contrast, Agrin-induced AChR clusters were significantly attenuated by antisense Dvl cDNAs (Figure 3C). Compared with vector-transfected myotubes, expression of antisense Dvl cDNAs inhibited Agrin-induced AChR clustering by 42%. Together, these results show that Dvl participates in Agrin/MuSK signaling that leads to AChR clustering. Because of the implication in AChR cluster stability, we determined whether receptor phosphorylation was

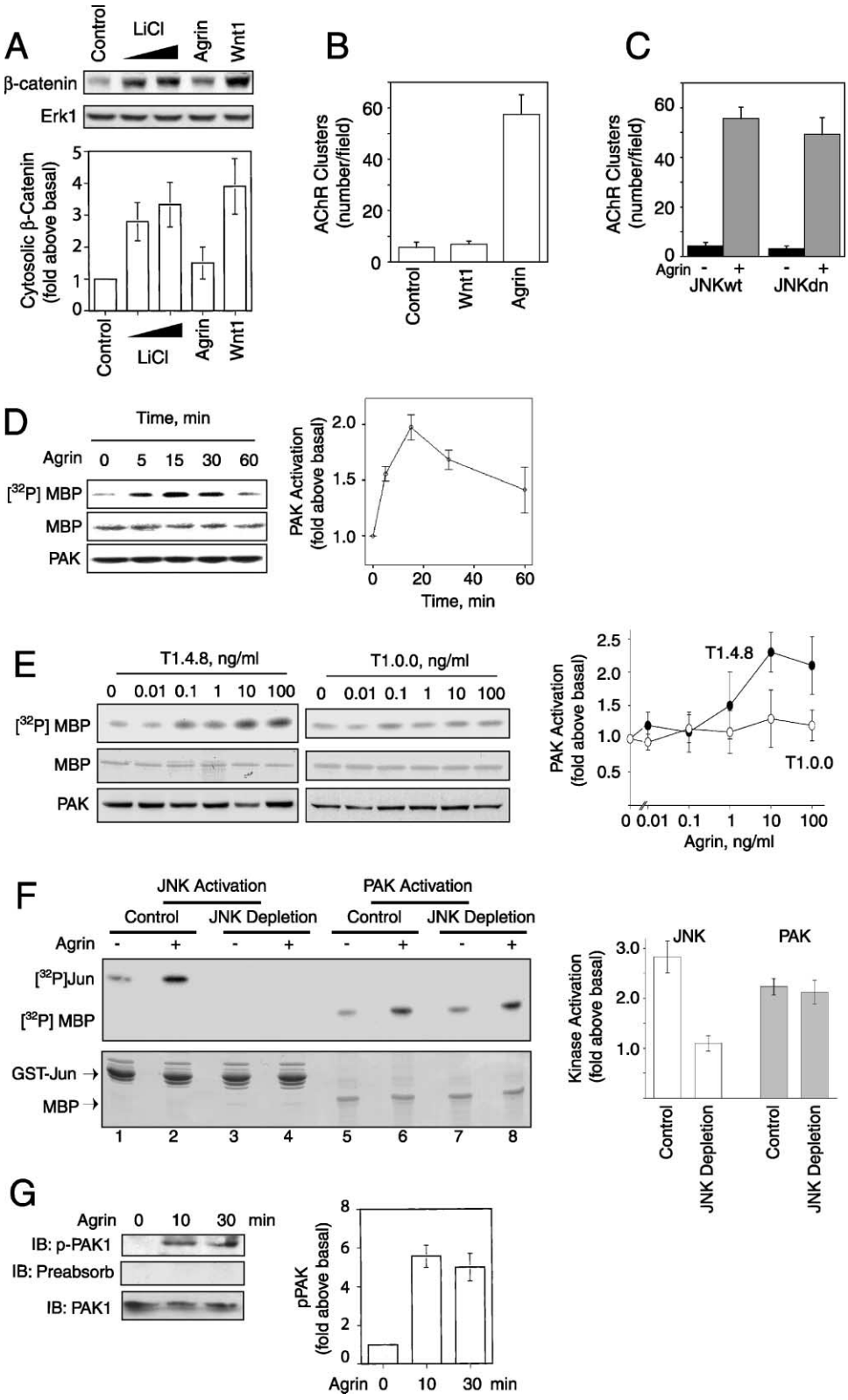

Figure 6. Agrin Activated PAK in Muscle Cells

(A) No effect of Agrin on cytosolic β-catenin. C2C12 myotubes were treated with vehicle (control), Wnt1 (Semenov et al., 2001), Agrin, or LiCl (3 and 10 mM) for 4 hr. Cytosolic proteins (30 μg) were subjected to immunoblotting with anti-β-catenin or anti-Erk antibodies (top panel). Densitometric analyses are shown in the histogram below.

(B) No effect of Wnt1 on AChR clustering. C2C12 myotubes were treated without or with Wnt1 or Agrin. AChR clusters were assayed as described in Figure 3. Data shown were means ± SEM (n = 3).

affected by DEP. In C2C12 myotubes infected with adenoviral DEP, AChR phosphorylation appeared to be decreased (Figure 3D), suggesting a mechanism by which Dvl regulates AChR clustering.

Dishevelled Regulates AChR Cluster Formation at Neuromuscular Synapses

To further characterize the role of Dvl in AChR clustering, we tested whether ΔDEP could inhibit Agrin-induced AChR clustering, using *Xenopus* nerve-muscle cocultures (Wang et al., 2001). Myc-Dvl or −ΔDEP mRNAs were injected together with GFP mRNA into one of *Xenopus* blastomeres at the two-cell stage. Muscle cells from injected embryos (stage 20) were cultured on glass coverslips. Cells overexpressing Myc-Dvl or −ΔDEP were identified by GFP fluorescence (Figure 4A). Immunocytochemistry using anti-Myc antibody confirmed that GFP fluorescence reflected faithfully expression of coinjected mRNA (31/34 Dvl-stained cells were GFP positive; all GFP cells were Dvl positive). Without Agrin, M^- myocytes (GFP negative) exhibited at most one to two large AChR clusters on their surface, and ΔDEP did not affect AChR clustering (Figures 4A and 4B). Agrin markedly increased the number of AChR clusters in control myocytes. In contrast, Agrin-induced AChR clustering was decreased in myocytes expressing ΔDEP (Figures 4A and 4B). Similar to our observations in C2C12 cells, expression of Dvl1 did not affect Agrin-induced AChR clustering (Figure 4B).

We next determined whether Dvl was involved in AChR clustering at the NMJ. In a triplet system shown in Figure 4C, a motoneuron innervated two muscle cells, one of which expressed ΔDEP (M^+) whereas the other did not (M^-). In comparison with controls (M^- myocytes), AChR clustering at M^+ synapses innervated by the same presynaptic neuron was hampered (Figure 4Cb). Quantitative analysis of pooled data from control ($n = 20$) and ΔDEP-expressing ($n = 18$) synapses indicated that expression of ΔDEP in the postsynaptic muscle cells significantly reduced the number, area, and intensity of AChR clusters (Figure 4D). Consistent with results in C2C12 cells and isolated myocytes (Figures 3 and 4B), postsynaptic expression of Dvl ($n = 18$) had no effect on AChR clustering (Figure 4D). Taken together, these results suggest that Dvl regulates the formation of AChR clusters at the developing neuromuscular synapses.

To determine whether the efficacy of synaptic transmission at the NMJ was altered by inhibition of Dvl signaling, we performed whole-cell voltage-clamped recording of action potential-independent, spontaneous synaptic currents (SSCs) on motoneuron-muscle cell triplets (Figure 5A). When ΔDEP (but not Dvl1) was expressed in postsynaptic cells (M^+ synapse), the amplitude of SSCs was significantly reduced as compared to the M^- synapse innervated by the same neuron (Figure 5B). The average amplitude of the SSCs declined by 50% in ΔDEP-expressing synapses (Figure 5C). A fall of SSC amplitude is expected when fewer AChRs are present in the postsynaptic site. However, there was no change in either the rise or decay time of SSCs, suggesting that the properties of AChR channels were not altered (Figure 5C). Unexpectedly, the frequency of SSCs was also decreased in ΔDEP-expressing synapses (Figure 5C). A decrease in SSC frequency usually reflects a reduction in presynaptic transmitter release, but a decrease in postsynaptic ACh responsiveness could also result in a lower SSC frequency, because some small-amplitude events are reduced to a level below the detection limits of recording (25 pA). In the later case, there should be a preferential decrease in small-amplitude events. However, the percentage of small-amplitude events (<50 pA) was not different between M^- and M^+ synapses (data not shown). Thus, perturbation of Dvl signaling in postsynaptic muscle cells not only inhibited AChR clustering, but also reduced transmitter release from the presynaptic terminals.

Involvement of PAK in Agrin-Induced AChR Clustering

MuSK shares a conserved extracellular cysteine-rich domain (CRD) with the Wnt receptor Frizzled (Dann et al., 2001; Masiakowski and Yancopoulos, 1998; Xu and Nusse, 1998). The finding that Dvl regulates Agrin-induced AChR clustering led us to determine whether the Wnt signaling pathways are involved in this event. As shown in Figure 6A, stimulation of C2C12 myotubes with Wnt1 and LiCl, an inhibitor of GSK3 (Klein and

(C) AChR clustering in JNK mutant cells. C2C12 cells that stably express wild-type or dominant-negative JNK (JNKdn) were stimulated with Agrin. AChR clusters were assayed as described in Figure 3. Data shown were means ± SEM ($n = 3$, $p > 0.05$).

(D) Agrin stimulation of PAK kinase in muscle cells. PAK1 was purified from Agrin-treated C2C12 myotubes and assayed in vitro for kinase activity with MBP as substrate in the presence of [γ-^{32}P]ATP. Radiolabeled MBP was resolved on SDS-PAGE and exposed to X-ray film (left panel). Amounts of MBP and PAK in the reaction were revealed by Coomassie staining and immunoblotting with the anti-PAK antibody, respectively. After exposure to X-ray film, MBP was cut out and counted for radioactivity. Data shown in the histogram were means ± SEM ($n = 4$).

(E) Dose-dependent PAK activation by neuronal but not muscle Agrin. Myotubes were stimulated with various concentrations of Agrin for 15 min. PAK1 activity was assayed as described in (D). The left panel shows representative radiogram and immunoblots. The histogram summarizes data (means ± SEM) from three experiments.

(F) JNK depletion had no effect on PAK activity. Myotubes were stimulated with 10 ng/ml Agrin for 15 min. Cell lysates were incubated with GST alone (control) or GST-Jun immobilized on agarose beads to deplete JNK and were assayed for PAK1 activity as described in (D) and JNK activity as described previously (Si et al., 1999). Amounts of GST-Jun were revealed by Coomassie staining. The left panel shows representative radiograms and immunoblots. After exposure to X-ray film, radiolabeled GST-Jun or MBP was cut out and counted for radioactivity. Data shown in the histogram were means ± SEM ($n = 3$).

(G) Detection of PAK1 activation by anti-phospho-PAK1 antibodies in muscle cells. Myotubes were stimulated with 10 ng/ml Agrin for 15 or 30 min. Cell lysates were blotted with anti-phospho-PAK1 antibodies or antibodies that were preincubated with the antigen. Amounts of PAK1 were revealed by immunoblot with anti-PAK1 antibody. The left panel shows representative immunoblots, and the histogram on the right summarizes densitometric analyses ($n = 3$).

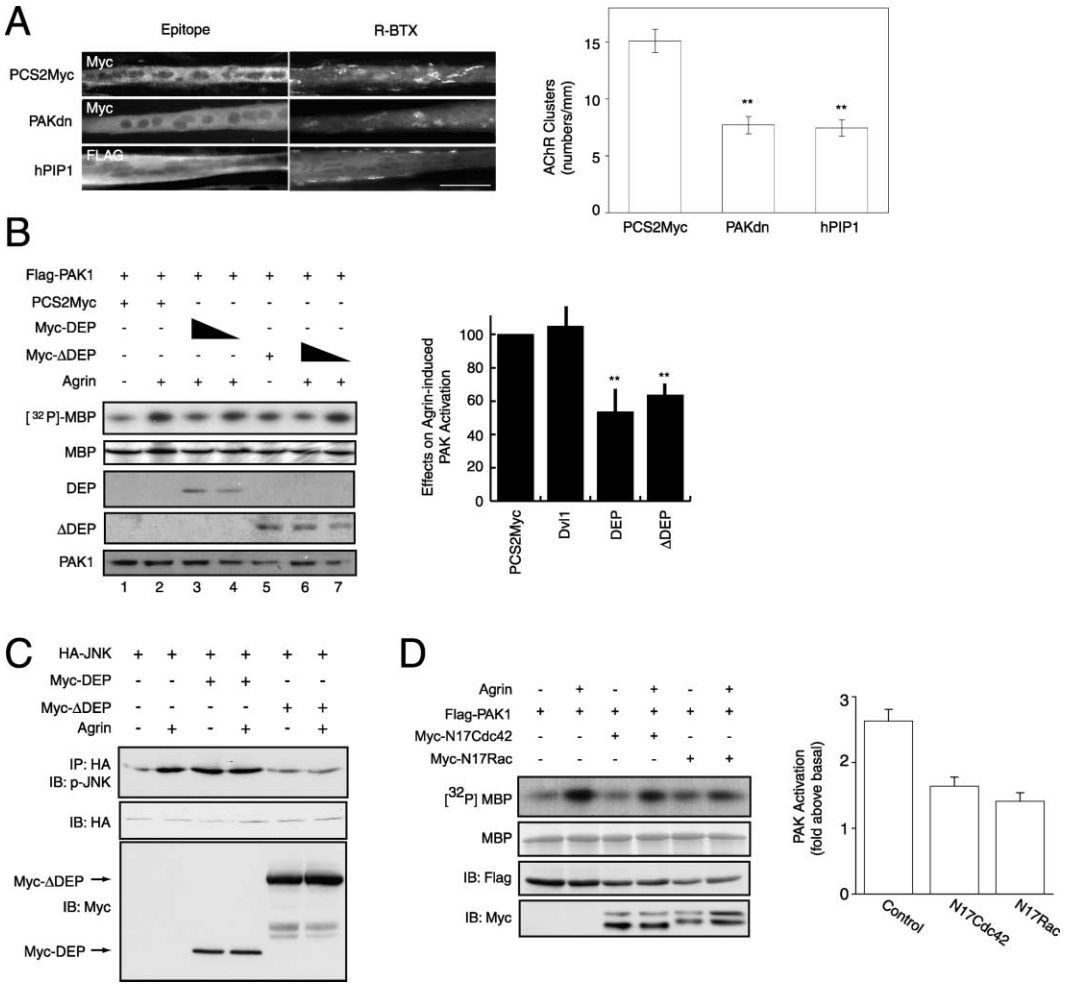

Figure 7. PAK Regulates Agrin-Induced AChR Clustering

(A) Inhibition of Agrin-induced AChR clusters by a PAK dominant-negative mutant and an inhibitor of PAK. C2C12 myoblasts were transfected with the empty vector, PAKdn, or hPIP1. Differentiated myotubes were treated with Agrin and stained with anti-Myc or Flag antibodies and R-BTX. Scale bar, 50 μm. The left panel shows representative images. The histogram summarizes data from numerous experiments (PCS2Myc, n = 29; PAKdn, n = 34; and hPIP1, n = 32). **$p < 0.01$, one-way ANOVA with Tukey HSD post hoc tests.

(B) Modulation of Agrin-mediated activation of PAK by Dvl mutants. C2C12 myoblasts were transfected with Flag-PAK1 without or with Dvl1 mutants. Myotubes were stimulated with Agrin, and PAK1 was purified by anti-Flag antibody and assayed as in Figure 6. Amounts of transfected proteins and MBP were shown by staining or immunoblotting. The left panel shows a representative radiogram and immunoblots. After exposure to X-ray film, ^{32}P-labeled MBP was cut out and counted for radioactivity. Data presented in the histogram are means ± SEM (n = 3), with Agrin-induced PAK activity in PCS2Myc myotubes as 100%. **$p < 0.01$, one-way ANOVA with Tukey HSD post hoc tests.

(C) Modulation of Agrin-mediated JNK activation by Dvl mutants. C2C12 myoblasts were transfected with HA-JNK without or with Dvl1 mutants. After stimulation with Agrin of differentiated myotubes, HA-JNK was purified by immunoprecipitation with anti-HA antibodies and probed with anti-phospho-JNK antibodies. Amounts of JNK and Dvl mutants were revealed by immunoblotting with anti-epitope antibodies.

(D) Dependence of PAK activation on Cdc42 and Rac. C2C12 myoblasts were transfected with Flag-PAK1 without or with dominant-negative Cdc42 or Rac mutants. After stimulation with Agrin of differentiated myotubes, PAK1 was purified by affinity chromatography using anti-Flag antibody and assayed for kinase activity as in Figure 6. Transfected proteins and MBP were shown by immunoblotting with respective antibodies. The left panel shows a representative radiogram and immunoblots. After exposure to X-ray film, ^{32}P-labeled MBP was cut out and counted for radioactivity. Data presented in the histogram are means ± SEM (n = 3), with Agrin-induced PAK activity in PCS2Myc myotubes as 100%. *$p < 0.05$, one-way ANOVA with Tukey HSD post hoc tests.

Melton, 1996; Stambolic et al., 1996), activated the canonical pathway as the cytosolic β-catenin was upregulated. The effect was not nonspecific because they had no effect on Erk. However, Agrin did not appear to affect β-catenin stability under the condition at which it increased AChR clusters (Figure 6A). These results suggest that Agrin did not activate the canonical pathway. In agreement, stimulation of myotubes with Wnt1 had no effect on AChR clustering (Figures 6A and 6B). These results suggest that the Wnt canonical pathway may not be involved in AChR clustering.

In addition to the canonical pathway, Dvl mediates the PCP pathway with increased Rho GTPase activity (Habas et al., 2001; Strutt et al., 1997). It has been shown that GTPases of the Rho family and cytoskeletal proteins play important roles in AChR clustering (Dai et al., 2000; Weston et al., 2000). Candidates of small GTPase effectors that regulate cytoskeleton include p21-activated

kinase (PAK), JNK, and proteins that regulate actin polymerization such as WASP and formin (Bishop and Hall, 2000). JNK is activated by Agrin in muscle cells (Weston et al., 2000) and by Dvl in a heterologous expression system (Boutros et al., 1998; Li et al., 1999). We have generated stable C2C12 muscle cells that express wild-type or dominant-negative JNK (Si et al., 1999). Neuregulin-induced expression of the ϵ subunit mRNA, which requires JNK activation, is inhibited in cells expressing dominant-negative JNK (Si et al., 1999). However, there was no significant difference in the number of Agrin-induced AChR clusters in C2C12 myotubes expressing wild-type or mutant JNK (Figure 6C). These results suggest that JNK activation may not be required for Agrin-induced formation of AChR clusters.

We next determined whether Agrin activated PAK in C2C12 myotubes. Stimulation of C2C12 myotubes with Agrin indeed increased PAK kinase activity in a time-dependent manner (Figure 6D). PAK activation by Agrin peaked at 15 min, to about 2-fold above basal. Muscle Agrin (T1.0.0), which is 1000-fold less potent in causing AChR clusters, had no apparent effect on PAK activity in C2C12 cells (Figure 6E). To exclude a possible contamination by JNK, which could be activated by Agrin, we characterized PAK activity before and after JNK depletion by GST-Jun. As shown in Figure 6F, JNK was activated 2.8-fold by Agrin (lanes 1 and 2). JNK activity was undetectable after JNK had been cleared from cell lysates (Figure 6F, lanes 3 and 4), indicating a complete depletion of JNK. However, the PAK activity was not significantly affected by JNK depletion (Figure 6F, lanes 5–8). To further characterize PAK activation by Agrin, we performed immunoblot analysis with the antibody that specifically recognizes activated PAK (Sells et al., 2000). Stimulation of C2C12 myotubes with Agrin led to a robust increase in PAK phosphorylation (Figure 6G). These results demonstrate that PAK is a downstream target of MuSK.

To investigate the role of PAK in AChR clustering, we studied the effect of a PAK dominant-negative mutant (K299R or PAKdn) whose kinase activity is abolished (Lei et al., 2000). The number of AChR clusters in PAKdn-expressing myotubes decreased 49% in comparison with controls, suggesting that disruption of PAK function inhibited AChR clustering (Figure 7A). To address further the importance of PAK, we determined whether AChR clustering is altered by hPIP1, a newly identified negative regulator of PAK and PAK signaling pathways (Kim et al., 2001; Xia et al., 2001). When expressed in C2C12 cells, hPIP1 effectively inhibited Agrin-induced AChR clustering (Figure 7A). These results demonstrate an important role of PAK1 in AChR clustering in response to Agrin.

Modulation of Agrin-Induced PAK Activation by Dvl

Our results suggest involvement of Dvl and PAK in Agrin-induced AChR clustering. Interacting with MuSK, Dvl may be positioned at the upstream of the pathway. Therefore, we explored the role of Dvl in Agrin-induced PAK activation. Agrin increased the activity of transfected Flag-PAK1 in C2C12 myotubes (lanes 1 and 2, Figure 7B). Dvl1 had no effect on Agrin-induced PAK activation (histogram, Figure 7B). However, Agrin-induced PAK1 activation was attenuated in C2C12 myotubes expressing Myc-DEP (Figure 7B, lanes 3 and 4) or Myc-ΔDEP (Figure 7B, lanes 6 and 7) in a concentration-dependent manner. These results demonstrate that Dvl is involved in Agrin-induced activation of PAK in muscle cells. Dvl mutants appeared to have distinct effects; in muscle cells expressing Myc-ΔDEP, Agrin was unable to increase JNK activity, suggesting that JNK activation may require Dvl (Figure 7C). The JNK activity in DEP-expressing cells, however, was elevated and did not increase further in response to Agrin. This result was in agreement of recent findings that Dvl activates JNK by DEP (Li et al., 1999). To delineate the relationship between GTPases and Agrin-induced PAK activation, we determined whether PAK activity was dependent on Cdc42 and Rac. Both dominant-negative mutants of Cdc42 and Rac attenuated PAK activation (Figure 7D). The inhibitory effect was more profound by N17Rac than N17Cdc42. These results indicate that PAK is downstream of Cdc42 and Rac.

A Ternary Complex of MuSK-Dvl-PAK

Having demonstrated the dependence of Agrin-induced PAK activation on Dvl, we sought to determine whether Dvl interacts with PAK. Myc-PAK1 coimmunoprecipitated with endogenous Dvl1 in HEK 293 cells, indicating that Dvl1 and PAK1 form a complex in mammalian cells (Figure 8A). Further analyses demonstrated that Dvl interacts with the p21 binding domain (PBD) in PAK (Figure 8B). In parallel experiments, PBD also bound to active but not inactive Cdc42, and GST alone did not associate with Dvl1. We next identified the domain in Dvl1 for PAK1 association. $Dvl1_{1–425}$, which contains both DIX and PDZ, coprecipitated with PBD (Figure 8C). In contrast, $Dvl1_{245–425}$, which contains PDZ and a partial DEP domain, did not interact with PBD, suggesting that PDZ is not required for interaction with PAK. In support of this finding, PBD also associates with $Dvl1_{1–260}$, which contains only DIX and the linker region between DIX and PDZ. These results suggest that PAK1 interacts with the N terminus of Dvl1.

The findings that MuSK interacts with DEP and PAK associates with the N terminus of Dvl raised the possibility that Dvl serves as an adaptor protein bridging PAK to MuSK in a ternary complex. To test this hypothesis, we screened for cells that express little or no endogenous Dvl to characterize possible interaction of MuSK with PAK with or without Dvl. HEK293, COS-7, and C2C12 cells all express relatively high levels of Dvl1 except quail fibroblasts (Figure 8D). Thus, quail fibroblasts were cotransfected with HA-MuSKic and/or Myc-Dvl1. Resulting lysates were incubated with GST-PAK1 immobilized on agarose beads to purify associated proteins. MuSKic alone did not interact with GST-PAK1 (lane 2, Figure 8E). Only when Dvl1-Myc was introduced was MuSKic detected in the precipitates by GST-PAK1. The MuSK-PAK1 association was dependent on the concentration of exogenous PAK1 (lanes 3–6, Figure 8E), but not GST (lane 1). In parallel experiments, PAK1 also associated with wild-type MuSK in the presence of Dvl (Figure 8F). These results indicate that Dvl1 promotes the association of MuSK with PAK1 as part of a ternary complex.

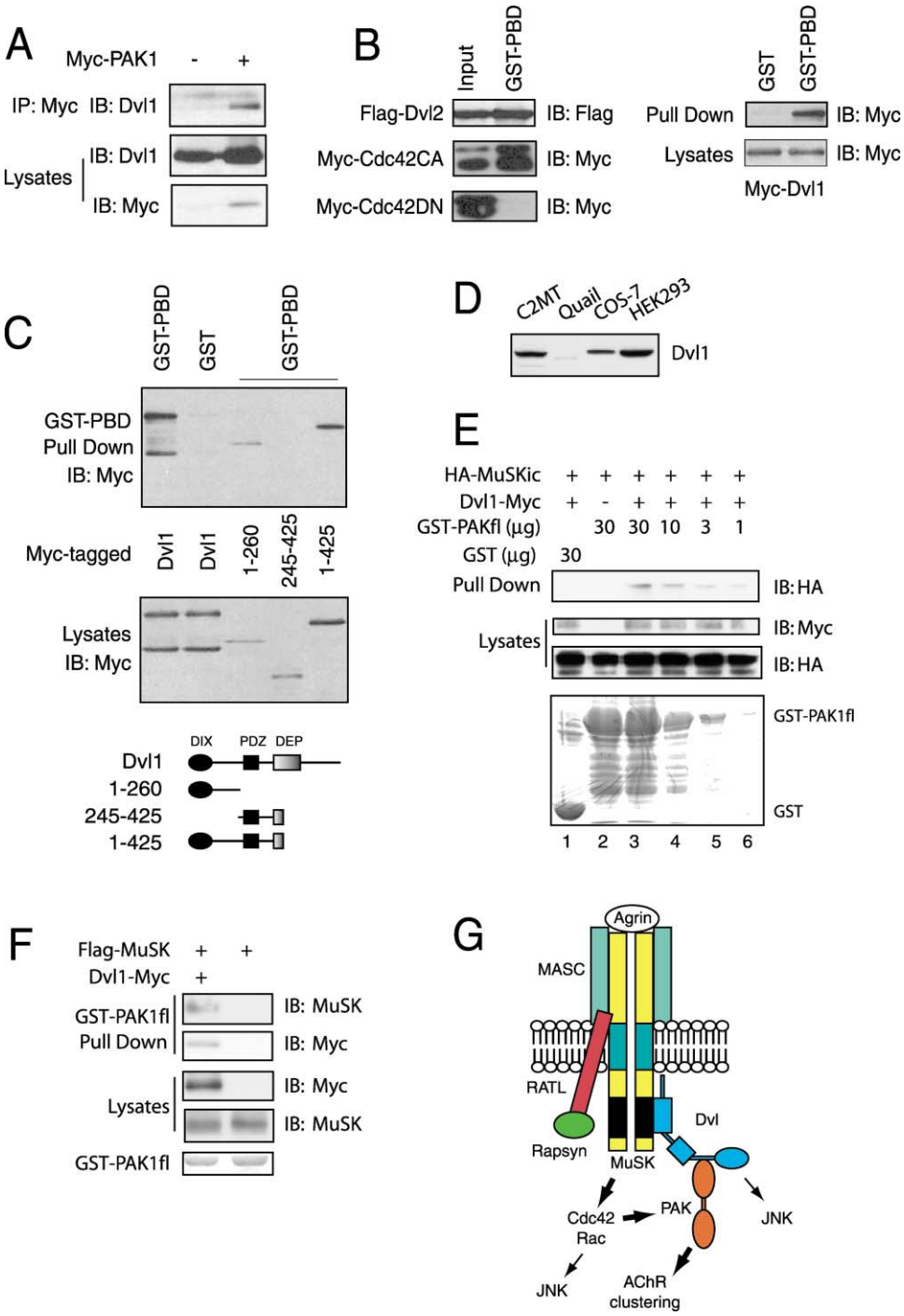

Figure 8. PAK Associates with MuSK in the Presence of Dvl

(A) Interaction of Dvl1 with PAK. HEK293 cells were transfected with Myc-PAK1. PAK1 was immunoprecipitated with anti-Myc antibody, and the resulting complex was probed with the anti-Dvl1 antibody.

(B) Interaction of Dvl with the PBD domain of PAK1. Lysates of cells expressing Flag-Dvl2, Myc-Cdc42CA, or Myc-Cdc42DN (left panels) and Myc-Dvl1 (right panels) were incubated with GST-PBD immobilized on beads. Bound proteins were subjected to immunoblotting with anti-Myc antibody.

(C) Interaction of PAK with the N-terminal region of Dvl1. Lysates of cells expressing Myc-tagged Dvl1 constructs were incubated with GST-PBD immobilized on beads. Bound proteins were subjected to immunoblotting with anti-Myc antibody. Lysates were also blotted to verify expression of respective Dvl1 constructs.

(D) Expression of Dvl1 in various cell lines. Lysates (20 μg protein) of indicated cells were immunoblotted for Dvl1.

(E) Ternary complex formation of MuSK, Dvl, and PAK. Quail fibroblasts were transfected with HA-MuSKic and/or Dvl1-Myc. Cell lysates were incubated with GST (control) or various concentrations of GST-PAK1 immobilized on beads. The resulting complex was probed with anti-HA antibody to detect MuSKic. Lysates were also blotted with indicated antibodies to verify expression of respective transfected proteins. GST and GST-PAK1 were demonstrated by Coomassie staining.

Discussion

There are two major findings in the present study. First, we show that MuSK interacts with Dvl. Disruption of the MuSK-Dvl interaction inhibits Agrin-induced AChR clustering in muscle cells and inhibits the formation of AChR clusters at the NMJ. Second, Dvl interacts with PAK1, which becomes activated in response to Agrin. We demonstrate that PAK activation requires Dvl, and inhibition of PAK1 activity attenuates AChR clustering. This study has identified Dvl as an important component in the Agrin/MuSK signaling pathway mediating AChR clustering at the NMJ. In this pathway, Dvl, by forming a scaffold with MuSK and PAK1, regulates AChR clustering. These results also provide evidence that impairment of AChR clustering inhibits presynaptic development at the NMJ.

MuSK and Dvl

The intracellular region of MuSK contains three domains: the juxtamembrane domain, the kinase domain, and the C terminus (Ganju et al., 1995; Valenzuela et al., 1995). The juxtamembrane and kinase domains appear to be involved in binding to Dvl. Deletion of either domain in MuSK leads to inability to interact with Dvl. These results suggest that either both domains contribute to the binding sites for Dvl or, alternatively, that one is essential for the proper conformation of the other. These results agree with data from recent structure-function analyses of MuSK revealing the importance of the juxtamembrane domain for MuSK activity (Herbst and Burden, 2000; Zhou et al., 1999). This domain is both necessary and sufficient to mediate Agrin-mediated AChR clustering (Herbst and Burden, 2000; Zhou et al., 1999). In a recent study, the juxtamembrane domains of EphB2 receptor tyrosine kinases are key to the proper conformation of the kinase domain (Wybenga-Groot et al., 2001).

The similarity between the extracellular domains of MuSK and Frizzled (Dann et al., 2001; Masiakowski and Yancopoulos, 1998; Xu and Nusse, 1998) suggests that Agrin may share the signaling pathways of Wnt. However, stimulation of myotubes with recombinant Wnt1 had no detectable effect on AChR clustering. On the other hand, we did not detect any Agrin-induced β-catenin upregulation, which occurs upon activation of the canonical Wnt signaling pathway. Furthermore, overexpression of Dvl, which increases the activity of JNK and PAR1 (Boutros et al., 1998; Fukumoto et al., 2001; Li et al., 1999; Sun et al., 2001), was unable to induce the formation of AChR clusters, suggesting that Dvl may not be sufficient for this event. These results, however, do not exclude the possibility that other Wnt signaling mechanisms are involved in AChR clustering. Alternatively, Agrin/MuSK-mediated AChR clustering is controlled by a novel Dvl-mediated pathway. As such, Dvl could serve as a signaling molecule at the crossroads of several divergent and convergent intracellular signaling pathways, including the canonical, PCP, and AChR clustering pathways. It is worth pointing out that our results do not rule out the possible involvement of other Wnt isoforms in AChR clustering.

In the mouse, three closely related *Dvl* genes have been identified (Klingensmith et al., 1996; Sussman et al., 1994; Tsang et al., 1996). They share 60%–70% overall identity in amino acid sequences. In addition, they are ubiquitously expressed during development, displaying extensive redundancy in spatial and temporal patterns of expression (Klingensmith et al., 1996; Sussman et al., 1994; Tsang et al., 1996). This suggests that there may be functional redundancy among these Dvl genes. All three members are expressed in muscle (Klingensmith et al., 1996; Pizzuti et al., 1996; Sussman et al., 1994) and interact with MuSK (this study and our unpublished data) and thus may be involved in mediating Agrin activity. *Dvl1*-deficient mice are viable and fertile with apparently normal structures including the NMJ (Lijam et al., 1997). As expected from these findings, Dvl1 mutant mice have normal NMJ (our unpublished data). Our inability to detect abnormal NMJs in these mice may be due to functional redundancy among different Dvl genes in the development of this structure. We will be able to test this hypothesis once Dvl2 and Dvl3 mutants are available.

AChR Clustering and Synaptic Differentiation

To fully qualify Dvl as a downstream molecule for Agrin/MuSK signaling, it is important to show that inhibition of its activity interferes with AChR clustering at the neuromuscular synapses. Our experiments using *Xenopus* nerve-muscle coculture demonstrate that this is indeed the case. Expression of mutant Dvl in the postsynaptic myocytes not only inhibited Agrin-induced AChR clustering in isolated muscle cells, but also the formation of AChR clusters at the NMJ. Interestingly, inhibition of synaptic AChR clusters reduced the amplitude as well as the frequency of spontaneous synaptic currents at the NMJ. These results provide strong evidence that impaired AChR clustering leads to attenuation of transmitter release. Since the Dvl mutant was selectively expressed in the postsynaptic myocytes, there may exist a muscle-derived, retrograde inhibitory signal that inhibits presynaptic transmitter release as a consequence of reduced postsynaptic AChR activity. Experiments using gene knockout mice demonstrated that disruption of AChR clustering in muscle cells is associated with se-

(F) Full-length MuSK interacts with PAK1 in the presence of Dvl1. Quail fibroblasts were transfected with Flag-MuSK and/or Dvl1-Myc. Cell lysates were incubated with GST-PAK1 immobilized on beads. The resulting complex was probed with anti-Flag antibody to detect MuSK. Lysates were also blotted with indicated antibodies to verify expression of respective transfected proteins. GST-PAK1 was demonstrated by Coomassie staining.

(G) A diagrammatic illustration of an intracellular pathway in Agrin/MuSK-mediated AChR clustering. Stimulation of MuSK with Agrin leads to activation of Cdc42 and Rac, which subsequently activate PAK. Dvl interacts with MuSK and PAK, forming a signaling scaffold important for Agrin/MuSK-mediated AChR clustering. Abbreviations: MASC, for muscle-associated specificity component; RATL, rapsyn-associated transmembrane linking molecule.

vere abnormalities in presynaptic motor axons at birth, including total absence or small size of terminal arborization (DeChiara et al., 1996; Gautam et al., 1995; Glass et al., 1996). Moreover, wild-type motor axons fail to form stable synaptic contacts with *rapsyn*$^{-/-}$ or *MuSK*$^{-/-}$ muscle cells transplanted in the wild-type host (Nguyen et al., 2000). These experiments indicate a role for AChR clustering in morphological differentiation of presynaptic terminals. An important finding in the present study is that inhibition of AChR clustering by postsynaptic expression of mutant Dvl resulted in a marked decrease in presynaptic transmitter release. Weakening of synaptic strength has been shown to be a prelude of axonal withdrawal during synaptic development (Colman et al., 1997). It is therefore conceivable that inhibition of Dvl signaling could ultimately lead to elimination of axonal terminals at the neuromuscular synapses. Moreover, these experiments raise the possibility that downregulation of MuSK/Dvl signaling may serve as a mechanism for synaptic elimination during development and synaptic atrophy in neuromuscular diseases.

A Signaling Pathway Regulating Agrin-Induced AChR Clustering

AChRs are associated with the F-actin cytoskeleton at the NMJ (Hoch et al., 1994). Actin polymerization may play an important role in the formation and/or stabilization of AChR clusters (Dai et al., 2000). How the actin cytoskeleton is regulated at the NMJ remains unclear. It is demonstrated that GTPases of the Rho family play an important role in regulating cytoskeleton (Bishop and Hall, 2000) and may regulate Agrin-induced AChR clustering. This hypothesis is supported by recent findings that Agrin stimulates Cdc42 and Rac in muscle cells, and dominant-negative Cdc42 and Rac inhibit AChR clustering (Weston et al., 2000). Moreover, small GTPases have been found to function downstream of Dvl (Boutros et al., 1998; Habas et al., 2001; Li et al., 1999; Strutt et al., 1997). In this study, we have explored role of two effectors of small GTPase that regulate cytoskeleton: PAK and JNK. Although JNK is activated by Agrin in muscle cells (Weston et al., 2000) and by Dvl in a heterologous expression system (Boutros et al., 1998; Li et al., 1999), it does not appear to regulate AChR clustering.

PAK is involved in Agrin-induced AChR clustering. First, Agrin activates PAK in cultured muscle cells. The activation is not nonspecific, because it is only elicited by neuronal, but not muscle, Agrin. Second, inhibition of PAK signaling by dominant-negative PAK or hPIP1 attenuates Agrin-induced AChR clustering. Moreover, PAK activation by Agrin is dependent on Cdc42 and Rac, suggesting that PAK may be downstream of the small GTPases. Exactly how these molecules interact with each other remains unclear. We show here that PAK, albeit unable to interact directly with MuSK, associates with it in the presence of Dvl, suggesting a multicomponent complex of MuSK, Dvl, and PAK. This complex may help to recruit PAK into the subsynaptic compartment for efficient PAK activation. In support of this hypothesis was the dependence of Agrin-induced PAK activation on Dvl function. Overexpression of Dvl mutants incapable of interacting with MuSK or PAK inhibited Agrin-induced PAK activity. Moreover, MuSK, Dvl, and phospho-PAK are enriched at the NMJ (our unpublished data). Taken together, these results led us to propose a working model in which Dvl functions as a scaffold protein bridging MuSK and PAK to form a multicomponent signaling complex (Figure 8G). In this pathway, activation of PAK by Cdc42 and Rac is facilitated. The complex may be important for the formation and maintenance of AChR clusters at the NMJ.

Experimental Procedures

Constructs and Antibodies

Dvl1 and mutants [1–160, 245–425, 1–425, and DEP (aa 380–504)] were subcloned into the ClaI site of pCS2+ in frame with 6-Myc epitope at the C termini. ΔDEP (Δaa 425–499) was constructed by Quickchange Site-Directed Mutagenesis Kit (Stratagene, La Jolla, CA). Flag-MuSK was generated by subcloning mouse MuSK in EcoRI/XbaI sites in pFlag-CMV1 downstream of an artificial signal peptide sequence and a Flag epitope. MuSKic was subcloned in the EcoRI site in pKH3 downstream of 3-HA epitope. GST-Dvl fusions were generated in pGEX2T (DIX, aa 1–100; PDZ, aa 245–345; and DEP, aa 404–504). Rabbit antisera were generated against the GST-Dvl1 C terminus (aa 599–695). Anti-p-PAK1 antibodies were from Santa Cruz and from Dr. Chernoff. Rabbit anti-MuSK antibody was from Dr. Ferns. Other antibodies were from Chemicon (actin), Santa Cruz (MuSK, PAK1, Myc, and HA), and Sigma (Flag).

Cell Culture, Transfection, and Biochemical Characterization

HEK 293 cells and C2C12 muscle cells were cultured and/or differentiated as described previously (Huang et al., 2000; Si et al., 1996, 1999; Won et al., 1999). Standard calcium phosphate technique was used for transfection. Cell lysates were prepared in a modified RIPA buffer including protease inhibitors (Huang et al., 2000, 2001). Immunoprecipitation and immunoblotting were performed as described previously (Won et al., 1999). Quantitative analyses of immunoblots were done using NIH image.

In Vitro Binding and ELISA

MuSK was in vitro translated with pMT-MuSK as a template using the T7/SP6 Coupled Reticulocyte Lysate System (Promega). ^{35}S-labeled MuSK was then incubated with GST-Dvl fusion proteins. Bound MuSK was resolved on SDS-PAGE and visualized by radiogram. For ELISA, His6/thio-tagged MuSKic and GST-Dvl constructs were purified from bacteria by TALON metal affinity resin (Clontech) and glutathione-sepharose, respectively. His6-MuSK protein (5 pmol/well) was coated to a 96-well plate in PBS for 12 hr at 4°C, washed, and blocked with 1% BSA in PBS for 6 hr at 4°C. Plates were incubated with GST-Dvl fusion proteins for 12 hr at 4°C, washed four times with PBS, and incubated with monoclonal anti-GST antibody for 2 hr at 4°C. After washing, plates were incubated with goat anti-mouse antibody conjugated with alkaline phosphatase for 2 hr at 4°C, washed, and subsequently incubated with 3 mM p-nitrophenyl phosphate in the substrate buffer containing 0.1 mM $MgCl_2$ and 5% diethanolamine (pH 9.8). The reaction was stopped with 1 N NaOH, and absorbance at 405 nm was determined with a microplate reader. The values were converted into relative binding with maximal absorbance as 100%.

AChR Clustering Assays

C2C12 cells plated on coverslips were transfected with or without indicated constructs. Fully differentiated myotubes were treated with 10 ng/ml Agrin (C4,8) for 18 hr to induce AChR clusters (Ferns et al., 1996). After fixation in 2% PFA for 30 min, cells were incubated with 50 nM R-BTX (Molecular Probes) for 60 min to label AChR and indicated antibodies to identify transfected myotubes. After incubation with FITC-conjugated secondary antibody, coverslips were mounted with VectaSheild (Vector Lab) and viewed under a Zeiss epifluoresence microscope. Images were collected with Openlab 3.0 software. AChR clusters whose diameters or longer axis was equal to or greater than 4 μm were scored.

AChR clusters in *Xenopus* muscle cells were labeled with R-BTX

as previously described (Wang et al., 2001). Briefly, 1-day-old nerve-muscle cultures were incubated with R-BTX for 45 min at room temperature, rinsed in PBS, and fixed with 3% PFA and 1% glutaraldehyde (EM Sciences) in PBS for 15 min. After brief rinses in PBS and H_2O, cells were mounted onto glass slides. AChR cluster images were acquired by a MicroMax 1300 cooled CCD camera (Roper Scientific) mounted on Nikon Diaphot 300 (1000 ms exposure time with a 60×, 1.40NA objective) and analyzed using IPLab software (Scanalytics). Pseudo-color green was assigned to fluorescent images of GFP. To quantify AChR clusters, we calculated background intensity by averaging the numbers obtained from three nonfluorescent areas on a muscle cell. The threshold was set for detecting fluorescent spots to four times above background intensity of that cell and normalized the fluorescent intensity of AChR clusters to background. The number, intensity, and area of the clusters were analyzed using the region-of-interest (ROI) tools in the IPLAB program (Version 3.7, Scanalytics, Inc.).

Adenoviral Infection and Phosphorylation of AChR β Subunit

Recombinant adenoviruses were generated as described previously (He et al., 1998). Briefly, DEP was cloned into pAdTrack-CMV. Ad-DEP and control AdGFP adenoviruses were generated in BJ5183 bacterial cells by homologous recombination of the viral pAdEasy-1 and pAdTrack-CMV-DEP and pAdTrack-CMV, respectively. 293 cells were used as hosts for viral production. C2C12 myotubes were infected with 100 MOI (multiplicity of infection) of control AdGFP or AdDEP virus. 24 hr after viral infection, cells were treated with 10 ng/ml Agrin for 1 hr and lysed in RIPA buffer. AChRs were isolated by α-BTX-conjugated sepharose 4B beads. Tyrosine phosphorylation of β subunits was detected using HRP-conjugated RC20 antibody (Transduction Laboratories). Membranes were reprobed using anti-β subunit antibody (Gillespie et al., 1996).

Xenopus Embryo Injection, Nerve-Muscle Cultures, and Electrophysiology

mRNAs of Dvl1 and ΔDEP were prepared using the mMessage mMachine kit (Ambion). *Xenopus* egg laying was induced by injecting a female *Xenopus* with human chorionic gonadotropin, and eggs were fertilized artificially with sperm derived from a male testis. mRNAs for DVL1 or ΔDEP (5 ng/μl in 1.5 nl) were mixed with GFP mRNA at 1:1 ratio and injected into one blastomere at the two-cell stage (Wang et al., 2001). Neural tubes and associated myotomal tissues of stage 20 embryos were dissociated in Ca^{2+}- and Mg^{2+}-free saline supplemented with EDTA (58.2 mM NaCl, 0.7 mM KCl, 0.3 mM EDTA [pH 7.4]) for 30 min. Isolated cells were cultured on glass coverslips for 24 hr at 23°C in medium consisting of (v/v) 50% Leibovitz L-15 medium (Sigma), 1% fetal calf serum (Life Technologies), and 49% Ringer's solution (115 mM NaCl, 2 mM $CaCl_2$, 2.5 mM KCl, 10 mM HEPES [pH 7.6]).

SSCs were recorded from innervated muscle cells by whole-cell recording methods at room temperature in culture medium (Lu et al., 1992). The solution in recording pipettes contained 150 mM KCl, 1 mM NaCl, 1 mM $MgCl_2$, and 10 mM HEPES buffer (pH 7.2). All data were collected in an event-triggering mode by a patch clamp amplifier (Axopatch 200B) with a current signal filter at 3 kHz. Data were stored on hard disk and a chart recorder (Gould EasyGraf 240) for offline analysis. Frequency, amplitude, and rise and decay times of SSCs were analyzed by Clampex (Version 8.0, Axon, Inc.).

Kinase Assays

C2C12 myotubes were harvested in the lysis buffer (50 mM HEPES [pH 7.4], 0.5 M NaCl, 5 mM $MgCl_2$, 0.5 mM EGTA, 50 mM NaF, 1% NP-40, 1 mM sodium vanadate, 1 mM PMSF, and 1 μg/ml each of pepstatin, leupeptin, and aprotinin). Cell lysates were cleaned by centrifugation and assayed for JNK activity as described previously (Si et al., 1999). To assay PAK1 activity, cell lysates were incubated with anti-PAK1 or anti-epitope antibodies immobilized on protein A beads at 4°C for 2 hr. After washing with the lysis buffer and then with the kinase buffer (50 mM HEPES [pH 7.4], 10 mM $MgCl_2$, 2 mM $MnCl_2$, 1 mM DTT), beads were incubated with 60 μl (final) of kinase buffer containing 10 μCi of [γ-^{32}P]ATP and 5 μg MBP at 30°C for 30 min. Phosphorylated MBP was resolved on 12% SDS-PAGE gels and visualized by radiogram. After exposure, MBP bands were excised and quantified using a Beckman scintillation counter.

Acknowledgments

We are grateful to Drs. S. Yanagawa, D. Sussman, J. Chernoff, M. Ferns, Z. Hall, R. Huganir, J. Chamberlain, and B. Vogelstein for valuable reagents; Drs. C. Garner and H. Wu for assistance with ELISA; Dr. Z.Z. Wang for sharing unpublished results; and NIH for grants to L.M., M.Y.L., Z.L., and X.H. A.W.B. is an EJLB Fellow and was supported by an institutional grant from HHMI. L.M. is a recipient of a HHMI/UAB Faculty Development Award.

Received: April 25, 2002
Revised: May 14, 2002

References

Axelrod, J.D., Miller, J.R., Shulman, J.M., Moon, R.T., and Perrimon, N. (1998). Differential recruitment of Dishevelled provides signaling specificity in the planar cell polarity and Wingless signaling pathways. Genes Dev. *12*, 2610–2622.

Bhanot, P., Brink, M., Samos, C.H., Hsieh, J.C., Wang, Y., Macke, J.P., Andrew, D., Nathans, J., and Nusse, R. (1996). A new member of the frizzled family from Drosophila functions as a Wingless receptor. Nature *382*, 225–230.

Bishop, A.L., and Hall, A. (2000). Rho GTPases and their effector proteins. Biochem. J. *348*, 241–255.

Borges, L.S., and Ferns, M. (2001). Agrin-induced phosphorylation of the acetylcholine receptor regulates cytoskeletal anchoring and clustering. J. Cell Biol. *153*, 1–12.

Borges, L.S., Lee, Y., and Ferns, M. (2002). Dual role for calcium in agrin signaling and acetylcholine receptor clustering. J. Neurobiol. *50*, 69–79.

Boutros, M., Paricio, N., Strutt, D.I., and Mlodzik, M. (1998). Dishevelled activates JNK and discriminates between JNK pathways in planar polarity and wingless signaling. Cell *94*, 109–118.

Burden, S.J. (1998). The formation of neuromuscular synapse. Genes Dev. *12*, 133–148.

Cadigan, K.M., and Nusse, R. (1997). Wnt signaling: a common theme in animal development. Genes Dev. *11*, 3286–3305.

Campanelli, J.T., Hoch, W., Rupp, F., Kreiner, T., and Scheller, R.H. (1991). Agrin mediates cell contact-induced acetylcholine receptor clustering. Cell *67*, 909–916.

Colledge, M., and Froehner, S.C. (1998). To muster a cluster: anchoring neurotransmitter receptors at synapses. Proc. Natl. Acad. Sci. USA *95*, 3341–3343.

Colman, H., Nabekura, J., and Lichtman, J.W. (1997). Alterations in synaptic strength preceding axon withdrawal. Science *275*, 356–361.

Dai, Z., Luo, X., Xie, H., and Peng, H.B. (2000). The actin-driven movement and formation of acetylcholine receptor clusters. J. Cell Biol. *150*, 1321–1334.

Dale, T.C. (1998). Signal transduction by the Wnt family of ligands. Biochem. J. *329*, 209–223.

Dann, C.E., Hsieh, J.C., Rattner, A., Sharma, D., Nathans, J., and Leahy, D.J. (2001). Insights into Wnt binding and signalling from the structures of two Frizzled cysteine-rich domains. Nature *412*, 86–90.

DeChiara, T.M., Bowen, D.C., Valenzuela, D.M., Simmons, M.V., Poueymirou, W.T., Thomas, S., Kinetz, E., Compton, D.L., Rojas, E., Park, J.S., et al. (1996). The receptor tyrosine kinase MuSK is required for neuromuscular junction formation in vivo. Cell *85*, 501–512.

Fallon, J.R., and Hall, Z.W. (1994). Building synapses: agrin and dystroglycan stick together. Trends Neurosci. *17*, 469–473.

Ferns, M., and Carbonetto, S. (2001). Challenging the neurocentric view of neuromuscular synapse formation. Neuron *30*, 311–314.

Ferns, M., Deiner, M., and Hall, Z. (1996). Agrin-induced acetylcho-

line receptor clustering in mammalian muscle requires tyrosine phosphorylation. J. Cell Biol. *132*, 937–944.

Fuhrer, C., and Hall, Z.W. (1996). Functional interaction of Src family kinases with the acetylcholine receptor in C2 myotubes. J. Biol. Chem. *271*, 32474–32481.

Fukumoto, S., Hsieh, C.M., Maemura, K., Layne, M.D., Yet, S.F., Lee, K.H., Matsui, T., Rosenzweig, A., Taylor, W.G., Rubin, J.S., et al. (2001). Akt participation in the Wnt signaling pathway through Dishevelled. J. Biol. Chem. *276*, 17479–17483.

Ganju, P., Walls, E., Brennan, J., and Reith, A.D. (1995). Cloning and developmental expression of Nsk2, a novel receptor tyrosine kinase implicated in skeletal myogenesis. Oncogene *11*, 281–290.

Gautam, M., Noakes, P.G., Mudd, J., Nichol, M., Chu, G.C., Sanes, J.R., and Merlie, J.P. (1995). Failure of postsynaptic specialization to develop at neuromuscular junctions of rapsyn-deficient mice. Nature *377*, 232–236.

Gautam, M., Noakes, P.G., Moscoso, L., Rupp, F., Scheller, R.H., Merlie, J.P., and Sanes, J.R. (1996). Defective neuromuscular synaptogenesis in agrin-deficient mutant mice. Cell *85*, 525–535.

Gillespie, S.K., Balasubramanian, S., Fung, E.T., and Huganir, R.L. (1996). Rapsyn clusters and activates the synapse-specific receptor tyrosine kinase MuSK. Neuron *16*, 953–962.

Glass, D.J., Bowen, D.C., Stitt, T.N., Radziejewski, C., Bruno, J., Ryan, T.E., Gies, D.R., Shah, S., Mattsson, K., Burden, S.J., et al. (1996). Agrin acts via a MuSK receptor complex. Cell *85*, 513–523.

Glass, D.J., Apel, E.D., Shah, S., Bowen, D.C., DeChiara, T.M., Stitt, T.N., Sanes, J.R., and Yancopoulos, G.D. (1997). Kinase domain of the muscle-specific receptor tyrosine kinase (MuSK) is sufficient for phosphorylation but not clustering of acetylcholine receptors: required role for the MuSK ectodomain? Proc. Natl. Acad. Sci. USA *94*, 8848–8853.

Habas, R., Kato, Y., and He, X. (2001). Wnt/Frizzled activation of Rho regulates vertebrate gastrulation and requires a novel Formin homology protein Daam1. Cell *107*, 843–854.

Hall, Z.W., and Sanes, J.R. (1993). Synaptic structure and development: the neuromuscular junction. Cell Suppl. *72* , 99–121.

He, T.C., Zhou, S., de Costa, L.T., Yu, J., Kinzler, K.W., and Vogelstein, B. (1998). A simplified system for generating recombinant adenoviruses. Proc. Natl. Acad. Sci. USA *95*, 2509–2514.

Herbst, R., and Burden, S.J. (2000). The juxtamembrane region of MuSK has a critical role in agrin-mediated signaling. EMBO J. *19*, 67–77.

Hoch, W., Campanelli, J.T., and Scheller, R.H. (1994). Agrin-induced clustering of acetylcholine receptors: a cytoskeletal link. J. Cell Biol. *126*, 1–4.

Huang, Y.Z., Won, S., Ali, D.W., Wang, Q., Tanowitz, M., Du, Q.S., Pelkey, K.A., Yang, D.J., Xiong, W.C., Salter, M.W., and Mei, L. (2000). Regulation of neuregulin signaling by PSD-95 interacting with ErbB4 at CNS synapses. Neuron *26*, 443–455.

Huang, Y.Z., Wang, Q., Xiong, W.C., and Mei, L. (2001). Erbin is a protein concentrated at postsynaptic membranes that interacts with PSD-95. J. Biol. Chem. *276*, 19318–19326.

Jennings, C.G., Dyer, S.M., and Burden, S.J. (1993). Muscle-specific trk-related receptor with a kringle domain defines a distinct class of receptor tyrosine kinases. Proc. Natl. Acad. Sci. USA *90*, 2895–2899.

Kim, H.W., Yang, P., Qyang, Y., Lai, H., Du, H., Henkel, J.S., Kumar, K., Bao, S., Liu, M., and Marcus, S. (2001). Genetic and molecular characterization of Skb15, a highly conserved inhibitor of the fission yeast PAK, Shk1. Mol. Cell *7*, 1095–1101.

Klein, P.S., and Melton, D.A. (1996). A molecular mechanism for the effect of lithium on development. Proc. Natl. Acad. Sci. USA *93*, 8455–8459.

Klingensmith, J., Nusse, R., and Perrimon, N. (1994). The Drosophila segment polarity gene dishevelled encodes a novel protein required for response to the wingless signal. Genes Dev. *8*, 118–130.

Klingensmith, J., Yang, Y., Axelrod, J.D., Beier, D.R., Perrimon, N., and Sussman, D.J. (1996). Conservation of dishevelled structure and function between flies and mice: isolation and characterization of Dvl2. Mech. Dev. *58*, 15–26.

Lei, M., Lu, W., Meng, W., Parrini, M.C., Eck, M.J., Mayer, B.J., and Harrison, S.C. (2000). Structure of PAK1 in an autoinhibited conformation reveals a multistage activation switch. Cell *102*, 387–397.

Li, L., Yuan, H., Xie, W., Mao, J., Caruso, A.M., McMahon, A., Sussman, D.J., and Wu, D. (1999). Dishevelled proteins lead to two signaling pathways. Regulation of LEF-1 and c-Jun N-terminal kinase in mammalian cells. J. Biol. Chem. *274*, 129–134.

Lijam, N., Paylor, R., McDonald, M.P., Crawley, J.N., Deng, C.X., Herrup, K., Stevens, K.E., Maccaferri, G., McBain, C.J., Sussman, D.J., and Wynshaw-Boris, A. (1997). Social interaction and sensorimotor gating abnormalities in mice lacking Dvl1. Cell *90*, 895–905.

Lin, W., Burgess, R.W., Dominguez, B., Pfaff, S.L., Sanes, J.R., and Lee, K.F. (2001). Distinct roles of nerve and muscle in postsynaptic differentiation of the neuromuscular synapse. Nature *410*, 1057–1064.

Lu, B., Greengard, P., and Poo, M.M. (1992). Exogenous synapsin I promotes functional maturation of developing neuromuscular synapses. Neuron *8*, 521–529.

Lumeng, C., Phelps, S., Crawford, G.E., Walden, P.D., Barald, K., and Chamberlain, J.S. (1999). Interactions between beta2-syntrophin and a family of microtubule-associated serine/threonine kinases. Nat. Neurosci. *2*, 611–617.

Malbon, C.C., Wang, H., and Moon, R.T. (2001). Wnt signaling and heterotrimeric G-proteins: strange bedfellows or a classic romance? Biochem. Biophys. Res. Commun. *287*, 589–593.

Masiakowski, P., and Yancopoulos, G.D. (1998). The Wnt receptor CRD domain is also found in MuSK and related orphan receptor tyrosine kinases. Curr. Biol. *8*, R407.

McMahan, U.J., Horton, S.E., Werle, M.J., Honig, L.S., Kroger, S., Ruegg, M.A., and Escher, G. (1992). Agrin isoforms and their role in synaptogenesis. Curr. Opin. Cell Biol. *4*, 869–874.

Megeath, L.J., and Fallon, J.R. (1998). Intracellular calcium regulates agrin-induced acetylcholine receptor clustering. J. Neurosci. *18*, 672–678.

Mohamed, A.S., Rivas-Plata, K.A., Kraas, J.R., Saleh, S.M., and Swope, S.L. (2001). Src-class kinases act within the agrin/MuSK pathway to regulate acetylcholine receptor phosphorylation, cytoskeletal anchoring, and clustering. J. Neurosci. *21*, 3806–3818.

Nguyen, Q.T., Son, Y.J., Sanes, J.R., and Lichtman, J.W. (2000). Nerve terminals form but fail to mature when postsynaptic differentiation is blocked: in vivo analysis using mammalian nerve-muscle chimeras. J. Neurosci. *20*, 6077–6086.

Noordermeer, J., Klingensmith, J., Perrimon, N., and Nusse, R. (1994). dishevelled and armadillo act in the wingless signalling pathway in Drosophila. Nature *367*, 80–83.

Perrimon, N., and Mahowald, A.P. (1987). Multiple functions of segment polarity genes in Drosophila. Dev. Biol. *119*, 587–600.

Pizzuti, A., Amati, F., Calabrese, G., Mari, A., Colosimo, A., Silani, V., Giardino, L., Ratti, A., Penso, D., Calza, L., et al. (1996). cDNA characterization and chromosomal mapping of two human homologues of the Drosophila dishevelled polarity gene. Hum. Mol. Genet. *5*, 953–958.

Qu, Z., and Huganir, R.L. (1994). Comparison of innervation and agrin-induced tyrosine phosphorylation. J. Neurosci. *14*, 6834–6841.

Ruegg, M.A., and Bixby, J.L. (1998). Agrin orchestrates synaptic differentiation at the vertebrate neuromuscular junction. Trends Neurosci. *21*, 22–27.

Sanes, J.R., and Lichtman, J.W. (1999). Development of the vertebrate neuromuscular junction. Annu. Rev. Neurosci. *22*, 389–442.

Sanes, J.R., and Lichtman, J.W. (2001). Induction, assembly, maturation and maintenance of a postsynaptic apparatus. Nat. Rev. Neurosci. *2*, 791–805.

Sells, M.A., Pfaff, A., and Chernoff, J. (2000). Temporal and spatial distribution of activated Pak1 in fibroblasts. J. Cell Biol. *151*, 1449–1458.

Semenov, M.V., Tamai, K., Brott, B.K., Kuhl, M., Sokol, S., and He, X. (2001). Head inducer Dickkopf-1 is a ligand for Wnt coreceptor LRP6. Curr. Biol. *11*, 951–961.

Si, J., Luo, Z., and Mei, L. (1996). Induction of acetylcholine receptor gene expression by ARIA requires activation of mitogen-activated protein kinase. J. Biol. Chem. *271*, 19752–19759.

Si, J., Wang, Q., and Mei, L. (1999). Essential roles of c-JUN and c-JUN N-terminal kinase (JNK) in neuregulin-increased expression of the acetylcholine receptor epsilon-subunit. J. Neurosci. *19*, 8489–8508.

Smith, C.L., Mittaud, P., Prescott, E.D., Fuhrer, C., and Burden, S.J. (2001). Src, Fyn, and Yes are not required for neuromuscular synapse formation but are necessary for stabilization of agrin-induced clusters of acetylcholine receptors. J. Neurosci. *21*, 3151–3160.

Stambolic, V., Ruel, L., and Woodgett, J.R. (1996). Lithium inhibits glycogen synthase kinase-3 activity and mimics wingless signalling in intact cells. Curr. Biol. *6*, 1664–1668.

Strutt, D.I., Weber, U., and Mlodzik, M. (1997). The role of RhoA in tissue polarity and Frizzled signalling. Nature *387*, 292–295.

Sun, T.Q., Lu, B., Feng, J.J., Reinhard, C., Jan, Y.N., Fantl, W.J., and Williams, L.T. (2001). PAR-1 is a Dishevelled-associated kinase and a positive regulator of Wnt signalling. Nat. Cell Biol. *3*, 628–636.

Sussman, D.J., Klingensmith, J., Salinas, P., Adams, P.S., Nusse, R., and Perrimon, N. (1994). Isolation and characterization of a mouse homolog of the Drosophila segment polarity gene dishevelled. Dev. Biol. *166*, 73–86.

Tanowitz, M.B., and Mei, L. (1996). Surgical denervation increases protein tyrosine phosphatase activity in skeletal muscle. Brain Res. *712*, 299–306.

Theisen, H., Purcell, J., Bennett, M., Kansagara, D., Syed, A., and Marsh, J. (1994). dishevelled is required during wingless signaling to establish both cell polarity and cell identity. Development *120*, 347–360.

Torres, R., Firestein, B.L., Dong, H.L., Staudinger, J., Olson, E.N., Huganir, R.L., Bredt, D.S., Gale, N.W., and Yancopoulos, G.D. (1998). PDZ proteins bind, cluster, and synaptically colocalize with Eph receptors and their ephrin ligands. Neuron *21*, 1453–1463.

Tsang, M., Lijam, N., Yang, Y., Beier, D.R., Wynshaw-Boris, A., and Sussman, D.J. (1996). Isolation and characterization of mouse dishevelled-3. Dev. Dyn. *207*, 253–262.

Tsim, K.W., Ruegg, M.A., Escher, G., Kroger, S., and McMahan, U.J. (1992). cDNA that encodes active agrin. Neuron *8*, 677–689.

Valenzuela, D.M., Stitt, T.N., DiStefano, P.S., Rojas, E., Mattsson, K., Compton, D.L., Nunez, L., Park, J.S., Stark, J.L., Gies, D.R., et al. (1995). Receptor tyrosine kinase specific for the skeletal muscle lineage: expression in embryonic muscle, at the neuromuscular junction, and after injury. Neuron *15*, 573–584.

Wallace, B.G. (1988). Regulation of agrin-induced acetylcholine receptor aggregation by Ca++ and phorbol ester. J. Cell Biol. *107*, 267–278.

Wallace, B.G. (1989). Agrin-induced specializations contain cytoplasmic, membrane, and extracellular matrix-associated components of the postsynaptic apparatus. J. Neurosci. *9*, 1294–1302.

Wallace, B.G., Qu, Z., and Huganir, R.L. (1991). Agrin induces phosphorylation of the nicotinic acetylcholine receptor. Neuron *6*, 869–878.

Wang, C.Y., Yang, F., He, X., Chow, A., Du, J., Russell, J.T., and Lu, B. (2001). Ca(2+) binding protein frequenin mediates GDNF-induced potentiation of Ca(2+) channels and transmitter release. Neuron *32*, 99–112.

Weston, C., Yee, B., Hod, E., and Prives, J. (2000). Agrin-induced acetylcholine receptor clustering is mediated by the small guanosine triphosphatases Rac and Cdc42. J. Cell Biol. *150*, 205–212.

Won, S., Si, J., Colledge, M., Ravichandran, K.S., Froehner, S.C., and Mei, L. (1999). Neuregulin-increased expression of AChR epsilon-subunit gene requires ErbB interaction with Shc. J. Neurochem. *73*, 2358–2368.

Wybenga-Groot, L.E., Baskin, B., Ong, S.H., Tong, J., Pawson, T., and Sicheri, F. (2001). Structural basis for autoinhibition of the Ephb2 receptor tyrosine kinase by the unphosphorylated juxtamembrane region. Cell *106*, 745–757.

Xia, C., Ma, W., Stafford, L.J., Marcus, S., Xiong, W.C., and Liu, M. (2001). Regulation of the p21-activated kinase (PAK) by a human Gbeta -like WD-repeat protein, hPIP1. Proc. Natl. Acad. Sci. USA *98*, 6174–6179.

Xu, Y.K., and Nusse, R. (1998). The Frizzled CRD domain is conserved in diverse proteins including several receptor tyrosine kinases. Curr. Biol. *8*, R405–406.

Yang, X., Li, W., Prescott, E.D., Burden, S.J., and Wang, J.C. (2000). DNA topoisomerase IIbeta and neural development. Science *287*, 131–134.

Yang, X., Arber, S., William, C., Li, L., Tanabe, Y., Jessell, T.M., Birchmeier, C., and Burden, S.J. (2001). Patterning of muscle acetylcholine receptor gene expression in the absence of motor innervation. Neuron *30*, 399–410.

Zhou, H., Glass, D.J., Yancopoulos, G.D., and Sanes, J.R. (1999). Distinct domains of MuSK mediate its abilities to induce and to associate with postsynaptic specializations. J. Cell Biol. *146*, 1133–1146.